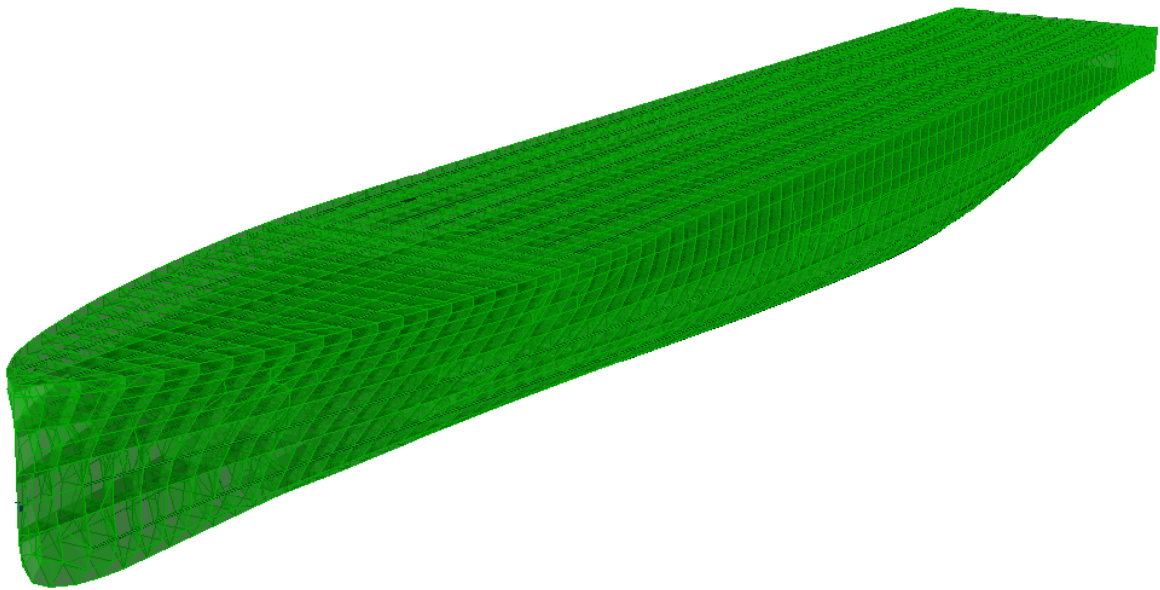




CHALMERS
UNIVERSITY OF TECHNOLOGY



Numerical Simulation Assessment of a Ship Dynamic Behavior Against a SSPA Model Test

Master's thesis in the International Master's Programme Naval Architecture and
Ocean Engineering

JAVIER PELAYO LLOP SAYSON

Department of Mechanics and Maritime Sciences
CHALMERS UNIVERSITY OF TECHNOLOGY
Gothenburg, Sweden 2019
Master's Thesis 2019/78

MASTER'S THESIS IN THE INTERNATIONAL MASTER'S PROGRAMME IN NAVAL
ARCHITECTURE AND OCEAN ENGINEERING

**Numerical Simulation Assessment of a Ship Dynamic
Behavior Against a SSPA Model Test**

JAVIER PELAYO LLOP SAYSON

Department of Mechanics and Maritime Sciences

Division of Marine Technology

CHALMERS UNIVERSITY OF TECHNOLOGY

Göteborg, Sweden 2019

Numerical Simulation Assessment of a Ship Dynamic Behavior Against a SSPA Model Test
JAVIER PELAYO LLOP SAYSON
© JAVIER PELAYO LLOP SAYSON, 2019

Master's Thesis 2019/78
Department of Mechanics and Maritime Sciences
Division of Marine Technology
Chalmers University of Technology
SE - 412 96 Göteborg
Sweden
Telephone: + 46 (0)31-772 1000

Cover: Hydrodynamic grid model using SESAM GeniE.

Printed by Chalmers Reproservice

Göteborg, Sweden 2019

Numerical Simulation Assessment of a Ship Dynamic Behavior Against a SSPA Model Test
Master's Thesis in the International Master's Programme in Naval Architecture and Ocean
Engineering

JAVIER PELAYO LLOP SAYSON

Department of Mechanics and Maritime Sciences

Division of Marine Technology

Chalmers University of Technology

Abstract

Shipping carbon emission impact will increase in the upcoming years, achieving more than 3% of CO₂ world emissions by 2030. It is not unthinkable of incoming regulations limiting these emissions. To affront this challenge, significant changes in ship performance and construction are heavily needed to minimize energy consumption. For that reason, there is a stronger need for more efficient and simplified methods in the prediction and analysis of ship energy efficiency and dynamic behavior. This thesis emphasizes the analysis and assessment of a ship's dynamic response to different sea states.

The objective of this thesis is to compare a state-of-the-art simulation model with a segmented model test carried out at the SSPA wave basin. The simulation model is created for its use in DNV GL's SESAM package software which assumed a rigid body motions model. SESAM GeniE has been used for the model calibrations, whereas Wasim SESAM is used in the seakeeping simulations.

The assessment of the model consisted of the use of modal analysis for the structural behaviour and seakeeping analysis for the wave loads response. The wet vibration analysis gave an accurate result of the segmented model, concluding that the numerical model structure captures the behavior of the hammer test.

The seakeeping simulations have proven good predictions on shear and bending moments, where the mean value is within 7% of the experimental value. It is concluded that with the current methodology and software, there is a satisfactory accuracy in the use of rigid numerical model to capture the vertical load behavior of a segmented experimental model in moderate sea states.

Keywords: experiments, numerical simulation, seakeeping, segmented model, wave basin.

Table of contents

Abstract	I
Table of contents	III
Preface	V
Nomenclature	VII
1 Introduction	1
1.1 Background and motivation of study	1
1.2 Objective and goals	3
1.3 Assumptions and limitations	3
1.4 Outline of thesis work	4
2 Methodology	5
3 Description of physical ship model tests	7
3.1 Segmented models	7
3.2 Experimental model of the case study vessel	9
3.2.1 Rigidity of the segmented model	10
3.3 Setup and design of the experiments	12
4 Description of the numerical simulation model	15
4.1 Wave definition	15
4.2 Hydrodynamic interaction with the hull	17
4.3 Setup of numerical simulations	18
5 Results and discussion	21
5.1 Calibration of the numerical model	21
5.2 Frequency analysis	22
5.2.1 Hammer test	22
5.2.2 Eigenfrequency analysis	23
5.3 Seakeeping simulations	26
5.3.1 Incident waves	27
5.3.2 Heave motions	28
5.3.3 Pitch motions	30
5.3.4 Roll motions	31
5.3.5 Shear forces	33
5.3.6 Vertical bending moments	36
5.3.7 Torsional bending moments	37
5.3.8 Discussion of results	39

6	Conclusions	41
7	Future work	43
9	References	45
Appendices:		
A.	Statistical data of the numerical and experimental results	49
A.1	S004	49
A.1.1	Condition 1	49
A.1.2	Condition 2	50
A.1.3	Condition 3	51
A.1.4	Condition 4	52
A.1.5	Condition 5	53
A.1.6	Condition 6	54
A.2	S005	56
A.2.1	Condition 7	56
A.3	S006	57
A.3.1	Condition 8	57
A.3.2	Condition 9	58
A.3.3	Condition 10	59
A.3.4	Condition 11	60
A.4	S007	61
A.4.1	Condition 12	61
A.5	S008	62
A.5.1	Condition 13	62
A.5.2	Condition 14	63
A.5.3	Condition 15	64
A.5.4	Condition 16	65

Preface

This thesis is part of the requirements for the master's degree in Naval Architecture and Ocean Engineering at Chalmers University of Technology, Göteborg, and has been carried out at the Division of Marine Technology, Department of Mechanics and Maritime Sciences, Chalmers University of Technology between January and June of 2019.

I want to acknowledge my examiner and supervisor Professor Jonas Ringsberg at the Division of Marine Technology on the Department of Mechanics and Maritime Sciences, Chalmers University of Technology for his knowledge, feedback, and encouragement. I also want to thank my co-supervisor Zhiyuan Li at Chalmers University of Technology for his support and guidance throughout all the thesis. I also like to give my gratitude to Olov Lundbäck from SSPA for his valuable time and feedback throughout the work.

Finally, I would send great gratitude to my family and friends for their endless support and love.

Göteborg, June 2019

Javier Pelayo Llop Sayson

Nomenclature

List of acronyms

BAU	Business as usual
CFD	Computational fluid dynamics
DOF	Degree of freedom
FE	Finite element
GHG	Greenhouse gas
HDF5	Hierarchical Data Format 5
IMO	International Maritime Organization
ITTC	International towing tank conference
JONSWAP	Joint North Sea Wave Project
MDL	Maritime Dynamics Laboratory
UN	United Nations

List of unit abbreviations

deg	degrees
kg	kilograms
Hz	hertz
m	meters
N	newton
s	seconds

Variables

<i>Ship dimensions</i>		<i>Unit</i>
B	Breath	m
D	Depth	m
T	Draft	m
LOA	Length overall	m
L_{pp}	Length between perpendiculars	m
LCB	Longitudinal center of buoyancy	m
LCG	Longitudinal center of gravity	m
m	Mass	kg
VCG	Vertical center of gravity	m
B_{wl}	Waterline breath	m
L_{wl}	Waterline length	m

<i>Wave properties</i>		<i>Unit</i>
γ	Phase angle	deg
A	Wave Amplitude	m
β	Wave direction	deg
H_s	Wave height	m
k	Wave number	-
T_s	Wave period	s

<i>Eigenanalysis</i>		<i>Unit</i>
ω_n	Natural frequencies	Hz
Γ	Correction factor dependent on the geometry of the beam.	-

1 Introduction

The following chapter presents the introduction to the thesis work. A detailed description of the background and motivation of the thesis presents the problem intended to be solved in the work. A list of assumptions and limitations is presented under which this problem will be addressed. Finally, an outline of the thesis work is done to present the different subjects addressed in this thesis.

1.1 Background and motivation of study

Shipping currently accounts for nearly 3% of global CO₂ emissions; by 2020 those emissions will increase by 7%. In 2030, the average emissions by the shipping industry will increase by 29% and by 2050 the increase will be around 95% of the ones in 2020. Thus, the shipping industry could end up being responsible for 17% of the CO₂ global emissions in 2050 if they were left unregulated (Smith et al. 2015).

The International Maritime Organization (IMO) has established a series of baselines for the amount of fuel each type of ship burns for a specific cargo capacity. It is expected that by 2025 all new ships will be 30% more energy efficient than those built in 2014. This, together with the progressively increasing highest regulations concerning energy efficiency will imply that the new build vessels of the future will inevitably be lighter in weight.

The projections of the emissions in the different planned scenarios done by the Third IMO GHG Study (2015) are displayed in Figure 1.1. The study argues that the improvements in efficiency mitigate the emissions growth, but even the most significant improvements modelled do not result in a downward trend. The study also defends that the primary source of this rise is due to the increasing demand for maritime transport. Putting then more pressure in the role of the maritime industry with GHG emissions.

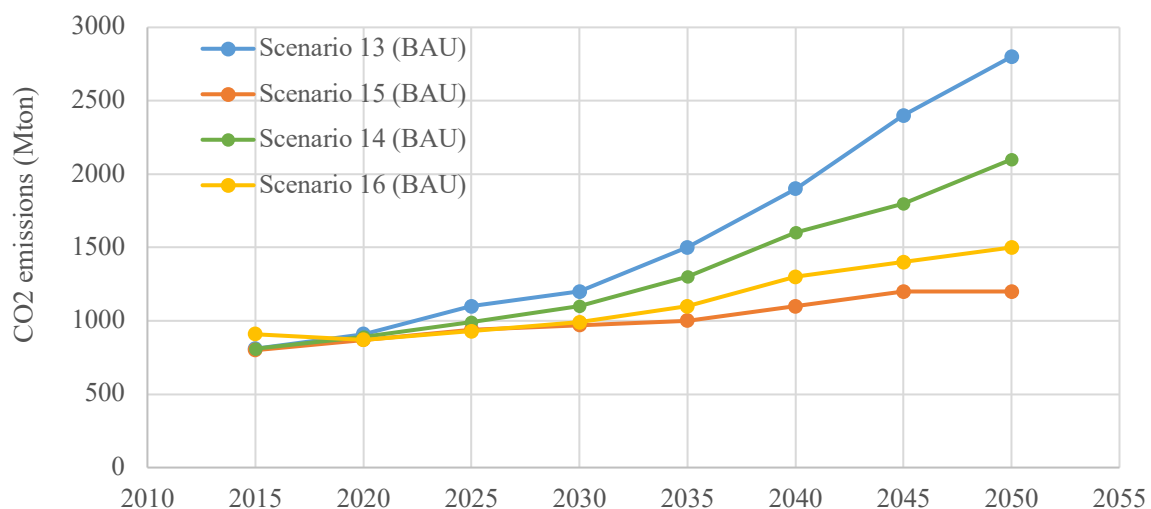


Figure 1.1: Emission projections for the BAU transport demand scenarios (Smith et al. 2015)

To avoid this situation the future vessels will need to move faster towards more sustainable transitions. The UN in their 2030 Agenda for Sustainable Development sets 17 Sustainable Development Goals; these goals integrate sustainable development in economic, social and environmental dimensions. (United Nations 2015). In the maritime industry, the IMO as the UN competent body gives advice and cooperation on how to move towards those goals. Of all the SDGs, the IMO takes a more interest concerning SDG 7 and SDG 13, concerning energy efficiency and the mitigation of climate change (IMO 2017). The IMO also promotes actions approaching the SDG 14 by the use of regulation of the carbon emission and marine geoengineering (IMO 2017).



Figure 1.2: The United Nation's 17 Sustainable Development Goals (United Nations 2019)

These challenges with the environment have motivated the urge for changes in shipbuilding. The intent of future designs is for increased energy efficiency, with the intent of complying with the environmental demands as well as for a more cost-effective vessel. One of the most popular developing methods to improve energy efficiency is by optimizing the hull design with a reduced weight. As a result of this optimization, the future new built vessels will have a more flexible hull, thus being more sensitive to waves. As a consequence, a hydroelasticity problem caused by the wave loads to the new, more efficient, vessel has to be addressed (Chen et al. 2017).

To ensure these optimizations do not compromise the structural integrity of the newbuilt vessel, new methods of hydrodynamic analysis have been developed. A more detailed experimental analysis that accounts for the new requirements can provide an insight into the dynamic load effect. Therefore, there is a tendency to simulate the complete vessel performance in waves instead of more focus-based single analysis in aspects such as rigid body response, slamming, sloshing or other areas of interest (Temarel et al. 2016).

At the same time, more simple methods of numerical analysis can give a faster and more robust solution, even if the applicability is limited due to the lack of critical physical phenomena not being considered. A more complete method has a more significant detail, but the solution

provided is more complex and time costly, making it not useful for some engineering applications. Additionally, in some cases it is not clear if the complex procedure can provide “better solutions” than a “simplified method”.

Under this situation, the Swedish Maritime Administration granted a project research, on which the division of Maritime Technology of Chalmers collaborates with SSPA and Stena to develop methods for dynamic designs of ship. The vessel used for this study is the next generation of RoPax vessel, Stena Elektra. Still in the concept stage, Stena Elektra is designed to be powered fully electric operating between Göteborg and Frederikshavn (Stena Teknik 2019).

In the joint project, model tests are conducted in SSPA’s towing tank, while the corresponding numerical simulations are carried out by Chalmers. In order to analyse better the behavior of the dynamic loads, SSPA carried out the experiments using a segmented or backbone model. Sophisticated numerical tools have been used to simulate the seakeeping characteristics and the dynamic structural responses of concept vessel. These have investigated together with the experimental data delivered by SSPA.

1.2 Objective and goals

The main objective of the thesis is to define under which circumstances can make a rigid body numerical model capture the behavior of a segmented backbone model. This is done by the use of a commercial tool and a state-of-the-art rigid body numerical model to simulate a sea basin experiment of a segmented backbone model.

An important goal is to understand under which sea state conditions and circumstances can make the simulation model capture the adequate motion and structural responses compared to a more flexible experimental model. This goal focuses on identifying where the limits are with the simulation model, under which conditions, and what needs to be adjusted and how in the simulation model.

Another goal of this thesis is to understand the methodology and behavior of the segmented model and to increase understanding and knowledge about dynamic loads on ship structures as well as the structural responses

The final goal is to define under which circumstances the numerical model data is similar to the experiment. Making it possible to deliver some recommendations on the use of a numerical dynamic model inside of the design process.

1.3 Assumptions and limitations

The main limitation of this thesis is the aim to predict the behavior of experiments done by a segmented backbone experimental model with a rigid numerical ship model. This will affect the comparison with the experimental data, because the more flexible segmented model is expected to be more sensitive to motions that will ultimately also affect the structure’s responses.

This assumption is based on the main objective of this work, and it is related to the software used for the simulations concerning the different properties of the SESAM software package (DNV 2006). This software package has been widely used in the assessment of the experimental test, but the simulations are assuming the ship to be a rigid body against the segmented model used in the experiments.

The dry condition eigenanalysis is done by SESAM GeniE (DNV GL 2015a) setting the limitations to the ones of the software's code. In this analysis the model is treated as a beam being dependent on the properties of its supports. This could affect the numerical interpretation of the free vibration causing then uncertainties with experimental model value.

The seakeeping simulations with SESAM HydroD (DNV GL 2016) follow the use of potential flow. A Rankine Panel method is chosen to define the fluid grid, and the irregular waves are defined by the JONSWAP spectrum. Linear wave theory has been used for all simulations expecting good prediction for all sea states; a limiting criterion may appear in harshest sea states where moderate nonlinear effects start to be introduced.

The experiments done by SSPA are not included in the thesis. Some particulars concerning the model and the test that are relevant for the assessment and analysis of the numerical results are introduced in further chapters. However, there are experimental uncertainties that have not been investigated. These together with the model uncertainties may cause deviation of the results, but they have not been studied in detail.

1.4 Outline of thesis work

The outline of this thesis is divided into seven different chapters. Chapter 2 presents the methodology of the work, the workflow as well as a presentation of the software used, and procedures followed. Chapter 3 describes the experimental methods where the relevant subjects of the experiments are presented, such as the type of model and the types of tests produced. The presentation of the use of numerical methods for dynamic behavior as well as the definition of the main characteristics of the simulation model is presented in Chapter 4. Chapter 5 presents and discusses the results of the simulations and their comparison with the experimental results. A conclusion is made in Chapter 6 where the results are summarized, and the main finding of the results are discussed. Recommendations for further work are presented in Chapter 7.

2 Methodology

The methodology and the workflow of this thesis can be found in Figure 2.1; the main theoretical concepts involving the numerical simulations are studied for an increased understanding of the results. After a calibration of the numerical model is carried out to simulate the experimental model. Numerical analysis has been carried out for the comparison and later assessment of the hull structure natural frequencies, ship motions and wave loads.

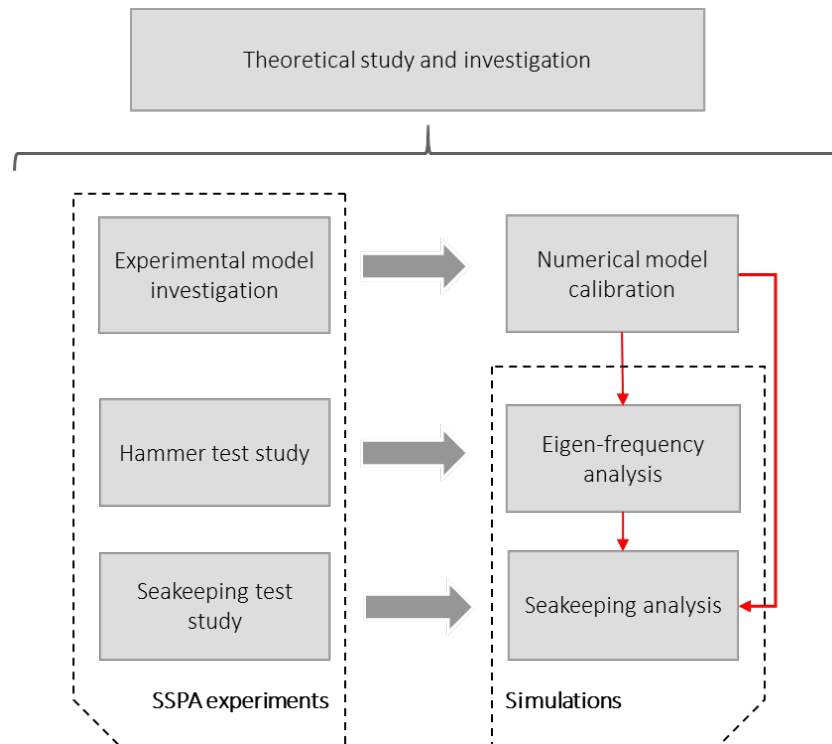


Figure 2.1: Chart describing the methodology applied in this thesis work

The theoretical study presented in this thesis is concerned with the limitations and assumptions of the thesis. An introduction to segmented models is presented as well as the main characteristics and properties in which this type of model functions. At the same time, the characteristics in which the simulations are defined are introduced. Concepts concerning the linearity of the waves, the panel method, and cross-section load calculation are presented. Also, the main particulars of the experimental test are presented in order to increase the understanding of the numerical analysis results.

The configurations of the numerical model are done using the package DNV GL SESAM. The eigenfrequency analysis is done using the FE-code Sestra inside DNV GL's SESAM GeniE (DNV GL 2015) while the hydrodynamic analysis is done with WASIM code inside HydroD (DNV GL 2016).

The scaling of the model test and experimental results are done following the ITTC Recommended Procedures and Guidelines (ITTC 2011). The dimensioning scale ratios for dynamic structural properties can be seen in Table 2.1.

A calibration of the numerical model is done to reproduce the test behavior. After, an eigenanalysis of the numerical model in FEM is implemented in dry and wet conditions in order to analyse the concerning model behavior and its later similarities with the experimental model.

Seakeeping simulations are also carried out following the main characteristics of the sea states, ship speeds, and wave direction according to the experiments. The ship motions for all these conditions are measured, as well as the cross-sectional forces and motions. These results are compared with the experimental data. These data are compiled in a series of HDF5 format files and data models that store the measured data of each one of the experiments runs. Each one of these hierarchical files contain all the relevant data for each experimental run, such as the moments, forces, wave spectrum and wave motions.

For the discussion and results, the extraction and statistical analysis of the results is done using MATLAB (Mathworks 2016). After, the conclusion to the thesis is presented. Finally, some recommendations for the use of the numerical model simulations as well as some proposed future work after the thesis.

Table 2.1: Ideal and Practical Scaling Ratios (Dinsenbacher et al. 2010)

Quantity	Prototype	Ideal Model	Practical Model
Length	L	L/λ	L/λ
Water density	ρ	ρ/c	ρ/c
Time	t	$t/\lambda^{1/2}$	$t/\lambda^{1/2}$
Mass	m	$m/c\lambda^3$	$m/c\lambda^3$
Velocity	v	$v/\lambda^{1/2}$	$v/\lambda^{1/2}$
Acceleration	a	a	a
Force	F	$F/c\lambda^3$	$F/c\lambda^3$
Ship Displacement	Δ	$\Delta/c\lambda^3$	$\Delta/c\lambda^3$
Moment	M	$M/c\lambda^4$	$M/c\lambda^4$
Pressure	P	$P/c\lambda$	$P/c\lambda$
Frequency (flexural modes and rigid body motions)	w	$w\lambda^{1/2}$	$w\lambda^{1/2}$
Bending Rigidity	EI	$EI/c\lambda^5$	$EI/c\lambda^5$
Shear Rigidity	KAG	$KAG/c\lambda^3$	$KAG/c\lambda^3$
Modulus of Elasticity	E	$E/c\lambda$	E/e
Section Area			
Moment of Inertia	I	I/λ^4	$Ie/c\lambda^5$
Distance from neutral axis to outermost fiber for hull-girder (prototype) or strength bar (model)	y	y/λ	y/r
Section modulus	Z	Z/λ^3	$Zer/c\lambda^5$
Flexure Stress	σ	$\sigma/c\lambda$	$\sigma\lambda/er$
Note: λ is the ratio of prototype to model length c is the ratio of prototype to water density e is the ratio of prototype to modulus of elasticity r is the ratio of distances from the neutral axis to the outermost fiber			

3 Description of physical ship model tests

In this chapter, the main characteristics of the experiments are presented. The particulars of the experimental model used are displayed as well as the main properties of a segmented model. The experiments carried out in the SSPA wave basin are also explained in order to provide knowledge for better numerical analysis and assessment of results presented later in the thesis. These experiments are the wave calibration, manoeuvring, hammer test, and seakeeping test.

3.1 Segmented models

The main particularity of the segmented model is that it can approach the hull interaction with waves as a hydro-elastic problem. On the other hand, the more general approach is to determine the ship loads and motions working on the assumption that the ship behaves as a rigid body (Jiao et al. 2019). This general assumption is not reliable enough for light weight vessels, high speed vessel or large ships where the wave loads and ship vibrations are considered as a hydro elastic problem. This hydro-elastic approach is proven to be better for fluid-structure interactions where the structure vibration and deformations are more accurate (Jiao et al. 2019).

The segmented model is characterized by dividing the ship’s model in several segments that are fixed by a beam or interface, also known as “backbone” (Figure 3.1). Segmented models transfer the wave forces on the hull to the backbone producing a better reading of the results, due to the hydro elasticity of the whole segmented model. Making their use ideal for seakeeping experiments, allowing them to investigate better hydro-elastic responses.

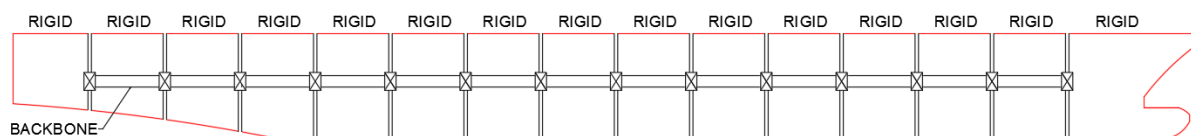


Figure 3.1: Sketch of a segmented body disposition

The segmented body simulates the model as a combination of smaller individual rigid segments and not as a whole rigid model, due to that it allows the segments to move individually in the six DOF (Figure 3.2). This allows it to be more prone to read the wave loads and their consequent phenomena, such as whipping and springing (Marón and Kapsenberg 2014). While the number of segments of the ship is determined by the desired detail of the results, the following rule of thumb can be made, the more modes shapes the higher number of segments (Marón and Kapsenberg 2014).

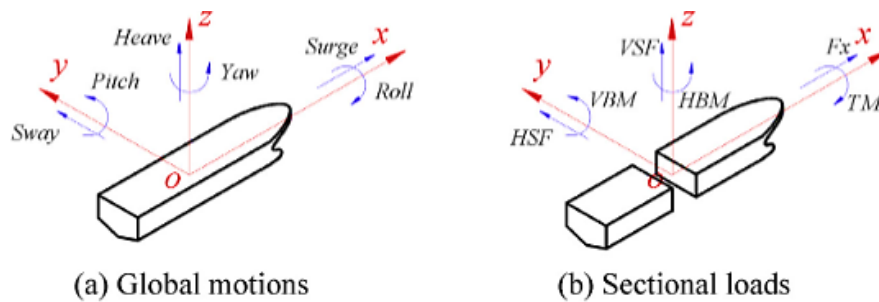


Figure 3.2: Definition of global motions and loads (Jiao et al. 2019)

The use of experimental models and their consequent numerical analysis has been widely used since 1980 (Davies et al. 2018). Since then, the segmented models have been mainly focused on the study of large containerships and bulk cargo vessels, due to their more sensible behavior towards horizontal wave loads, therefore having also higher probabilities on whipping and springing.

These effects are a consequence of the dynamic interaction between ship and wave both in dynamic mode. The impact of the waves into a moving ship usually does not suppose a greater effect into the hull structure, but in rough weather when slamming occurs (produced by the sudden impact of the bow when it breaks away from the water) it can excite the structure producing whipping. Whipping is, as a consequence of slamming, a two-node vibration of the hull on fundamental frequency that can produce high stresses and large loads in the area of impact.

Springing, which is also a result of the interaction between the structure and the waves, is the resonance between the frequencies of the waves encounter and the natural frequency of the ship. Slamming, as well as whipping, can be avoided by reducing the speed or changing the course of the vessel. Unfortunately, it is more difficult to predict springing due to all the different wave frequencies that can be found in several sea states. That is why a proper investigation of the structure natural frequencies in the model is really important for the ship's behavior.

For most of the segmented models the space between the cuts of each segment is usually between 5 to 10 mm. The use of rubber for the model construction is not recommended because of its disturbance in high damping (Storhaug 2014). For investigation, the model has to share the same neutral axis as the real ship. The elasticity of the model depends on a high degree on the stiffness of the backbone. From the rigidity of the backbone, a segmented model can be divided into two types: elastic and rigid (ITTC 2011).

1. **Rigid Segmented model.** This type of segmented model is characterized by having a much more rigid backbone. In this model there is no variation on the wave peaks at measured and natural structural frequencies making them larger than the wave frequency (ITTC 2011). Load data can evaluate either from each segment or directly from the bending moment from the beam. For the eigenanalysis, the model can be assumed to be rigid making it able to use its loading results as an input for an analysis of the structure. (ITTC 2011).

2. **Elastic Segmented model.** This type of segmented model is characterized by having an elastic backbone, allowing to read the different data at different points of the model. A rigid internal structure can be used in these types of models in which the rigidity of the model segments can be instrumented (ITTC 2011).

Segmented models are made to reproduce the vibrations in the most realistic way, generally for vertically in two nodes modes. Depending on the purpose of the study such as in the investigation of a refinement the model's material is made and by matching the natural frequencies, using an open section beam, the analysis can be done (Hong et al. 2011). The mass distribution of the model should be following the same mass properties as the ship under study. For fatigue analysis, where the whipping and springing are analysed, it is recommended to have three flexible joints in the model (Storhaug 2014).

For the experimental test, the model can be moved either self-propelled or towed externally. In the case of being towed, the towing forces cannot interfere with the experiments. The springs supporting the model should give real values for surge and model speed and at the same time not compromise the direction (Storhaug 2014).

3.2 Experimental model of the case study vessel

The model is an elastic segmented model divided into four different segments (Figure 3.3), which ensures a proper reading of the data and at the same time, makes it more economically viable. Each segment had a stiff carbon fibre box that with the use of adjustable springs on the top of the model could change the flexibility of the model.

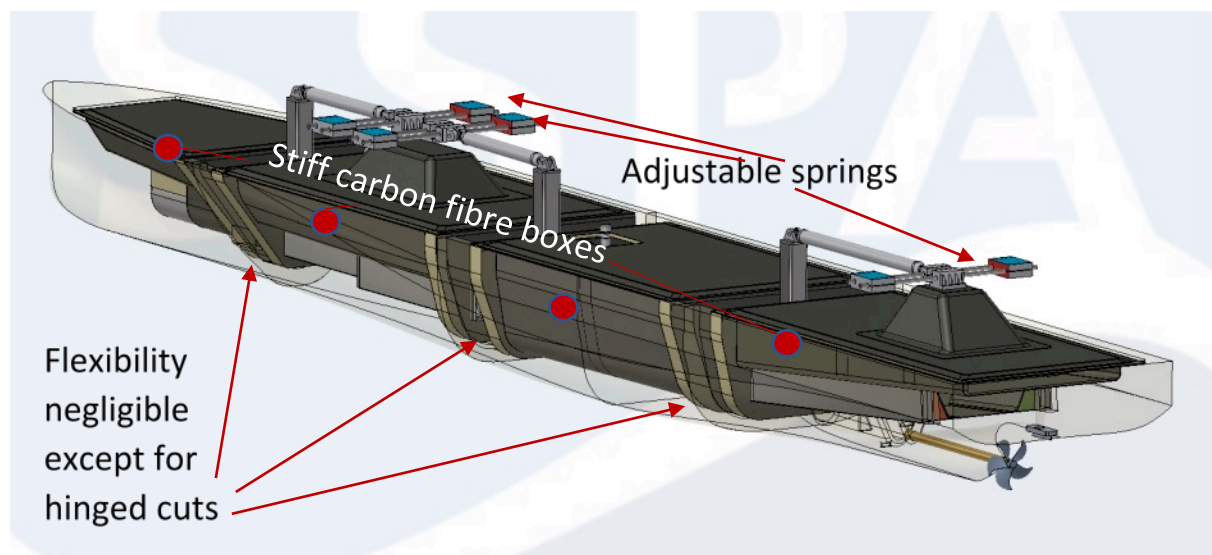


Figure 3.3: Experimental model set up

The main particulars model and their respective scaled value for the full-size vessel are displayed in Table 3.1. These characteristics and properties of the model are scaled to full size to be fitted for the numerical simulation in order to ensure that the properties of the experiment stay the same in the computational simulations, following the ITTC scale recommendation shown in Table 2.1.

Table 3.1: Model characteristics

Model	Experimental	Numerical
Length between perpendiculars, L_{pp} [m]	5.284	195.5
Waterline length, L_{wl} [m]	5.072	187.68
Depth, T [m]	0.409	15.12
Beam, B [m]	0.749	27.74
Beam in waterline, B_{wl} [m]	0.715	26.46
Draught fore [m]	0.17	6.3
Draught aft [m]	0.17	6.3
Displacement, Δ [kg]	356.69	18 477 075
LCB, LCG [m]	2.405	88.985
VCG [m]	0.314	11.61
Water density [kg/m ³]	998	1025
Water ratio density		0.97
Scale factor		37

For the reading of the data, the coordinate system for the experiment follows x- horizontal, y- transversal, z- vertical; being the positive direction looking at the fore-ship and into the bottom. The center of gravity is set at the aft perpendicular at ground level. The measuring cross-section is located at the aft, fore, and mid-section of the model at 6.29 meters from the ship base. In this work only the midsection data has been analysed, being the measuring point coordinates located at (88.895, 0, 6.29) meters.

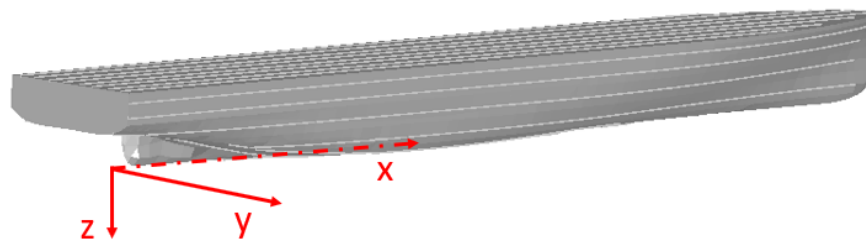


Figure 3.4: Coordinate system

3.2.1 Rigidity of the segmented model

A segmented model such as the one used can predict the eigenfrequencies by adjusting the mass distribution and effective stiffness. This gives the model four degrees of freedom for each segment (the three direction displacements (x, y, z plus the horizontal rotation of the hull segment). Therefore, the model is able to reproduce the flexural dynamics of the real vessel (Vakilabadi et al. 2014).

The weight distribution of the model as presented by SSPA is in Figure 3.5. There, the center of gravity and moments of inertia of each segment are set in order to the full size vessel in full operation. The stiffness of the model was set to reach a target stiffness of 2442 Nm/deg for all

three cuts of the model. These results can be seen in Table 3.2, whereas the total stiffness distribution in the model is displayed in Figure 3.6.

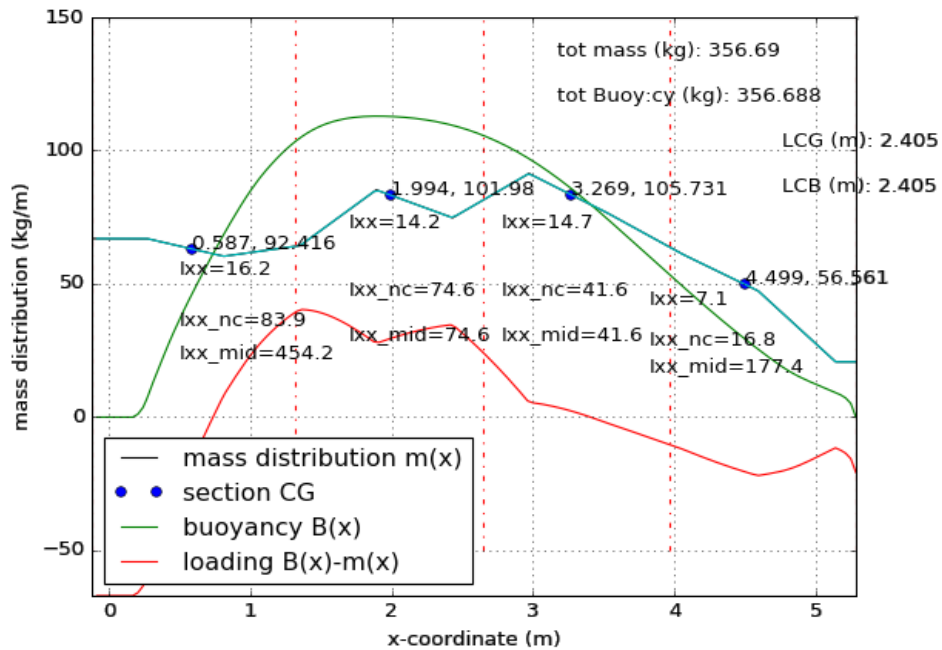


Figure 3.5: Graph over mass distribution, buoyancy distribution (model scale)

Table 3.2: Achieved values of cut stiffness

Cut	Stiffness (Nm/deg)
Aft	2452
Mid	2522
Fore	2397

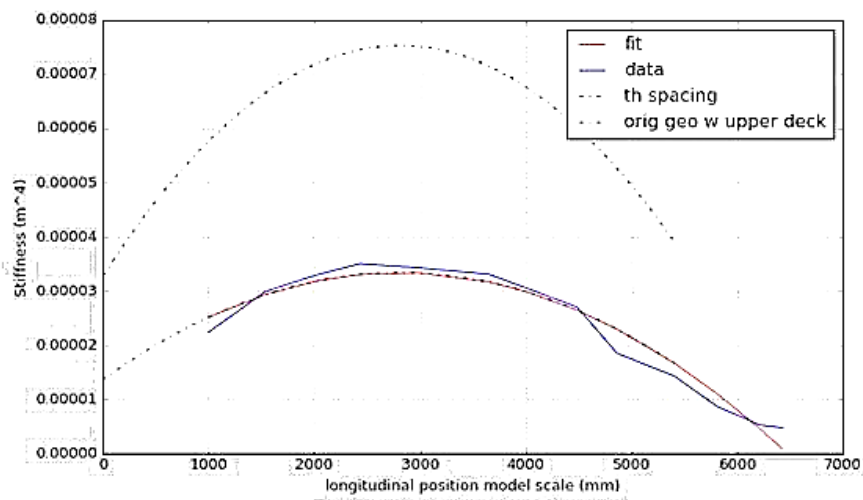


Figure 3.6: Stiffness distribution model scale

3.3 Setup and design of the experiments

To understand the hydrodynamic behavior the structural integrity of the vessel under dynamic loads, SSPA carried out the experiments under a segmented or backbone experimental model. This will make it possible to provide data for analysis in the following areas of interest (ITTC 2011):

1. Primary design loads
2. Slamming, whipping and springing loads
3. Validation of computational methods
4. Frequency domain application to lifetime designs
5. Application to extreme loads – stochastic analysis
6. Fatigue analysis and design
7. Safe operating envelope

The focus of this project lays in the validation of the computational methods, giving later some recommendations for the use of the model for the rest of the areas of interest.

The SSPA different experiments can be summarized in Table 3.4; these experiments consist of a series of different types that go from the wave basin and model calibration to the seakeeping experiments. These different test types carried out with the model are:

- 1) **Wave calibration:** For the preparation of the tank a wave calibration is needed in order to set the different sea states for other test types. For each different run, the wave height and wave period has been measured to ensure their quality.
- 2) **Manoeuvring:** Preparation test done in order to calculate the GM and to do the model speed calibration for all the different speeds.
- 3) **Hammer test:** Test that consists of hitting the model with a hammer to see the resonance frequency of the model structure. This type of test was carried out in dry and wet conditions.
- 4) **Seakeeping:** These tests are carried out using the JONSWAP spectrum in the wave basin, they were done with following seas and bow seas (180 and 150 degrees) at different speeds in order to increase the number of wave encounters and increase the chance of slamming.

The wave calibration and manoeuvring form part of the set up for the preparation of the wave basin for the seakeeping test these two tests are not relevant to the simulations but are essential for the preparation of the experiment. The wave calibration is the set-up of each of the different sea states in the basin for a period of time, ensuring the wave behavior for the next experiments. The calibration of the waves had a duration of 10 minutes per sea states; the different sea states can be shown in Table 3.3. On the other hand, the manoeuvring test consists of the calibration of the model speed in the wave basin in order to ensure the behavior of the model for further experiments.

The seakeeping test are then divided into different series, each one representing one of the different five sea states. These sea conditions are representative of the area of the operation of the real vessel. The last two seakeeping series are neglect due to their lack of providing any relevant information. In S009 there was no performance of the model, while S010 failed to provide any added data concerning the aft-body slamming in following seas.

Table 3.3: Test series sea states

Series	Sea state	Hs [m]	Tp [s]
S004	4 long crested seas	1.88	7.56
S005	4 short crested seas	1.88	4
S006	5 long crested seas	3.25	9.24
S007	5 long crested seas	3.25	5
S008	6 long crested seas	5	10.78

The waves generated for all the seakeeping tests are irregular; this type of wave is suited to determine unknown resonances, response amplitude operator and statistical data provided from the time series data. The selection of short crested seas for S005 and S007 helps to provide a higher loading impacting the model. The calmer sea states, from series S004 to S006, are expected to behave well inside the linear wave theory, while the in rougher sea states, for series S007 and S008, the behavior is expected to be within the border of nonlinearity.



Figure 3.7: Seakeeping test run in SSPA MDL wave basin

To make the comparison with the numerical simulations, a compilation of relevant data from different model tests has been assembled for each simulated condition. That way, the resultant

assembled test data for each condition has had more experimental time to compare against the numerical simulations. The total experimental time for each simulation condition that has been compared against the simulation are presented in Table 4.3. The experiments test selected and compiled for each condition that have been compiled for the assessment of this thesis can be found in the appendix.

Table 3.4: Experiments run set up

Series	Test type	Number of tests	Sea states	Wave direction [deg]	Model speed [m/s]	Ship speed [kts]
S000	Wave calibration	5	--	--	--	--
S001	Manoeuvring	10	--	--	--	--
S003	Hammer test and control	--	--	--	--	--
S004	Seakeeping	28	4 long crested seas	150; 180	1.269; 1.522; 1.776	15; 18; 21
S005	Seakeeping	9	4 short crested seas	180	1.522	18
S006	Seakeeping	23	5 long crested seas	150; 180	1.269; 1.522	15; 18
S007	Seakeeping	9	5 long crested seas	180	1.522	18
S008	Seakeeping	11	6 long crested seas	150; 180	1.015; 1.269	12; 15
S009	Seakeeping	--	--	--	--	--
S010	Seakeeping	--	--	--	--	--

4 Description of the numerical simulation model

The aim of this chapter is to describe the theoretical basis for the software and models. Theoretical concepts regarding the assumptions and limitations for the wave grid and the calculation of forces and motion give later a large understanding of the numerical results against the experiment data. Later, the set up for the simulation are presented, showing the main defining characteristics for the seakeeping simulation.

4.1 Wave definition

The wave definition has been done using the Wasim interface inside SESAM HydroD (DNV GL 2016). Showing that the waves can be described as the sum of harmonics defined as (DNV 2006):

$$\eta(x, y, t) = A \cos[(k \cos \beta)x + (k \sin \beta)y - \omega t + \gamma] \quad (1)$$

Which can also be expressed in complex form as;

$$\eta(x, y, t) = A \exp [i((k \cos \beta)x + (k \sin \beta)y - \omega t + \gamma)] \quad (2)$$

The use of wave amplitude and phase angle as parameters in the sum of harmonics allows to define all types of sea states. At the same time, Wasim allows the possibility of using infinite depth, which would allow the term:

$$k = \frac{\omega^2}{g} \quad (3)$$

The wave grid in Wasim is done using the Rankine Panel method; one of the advantages of this method is its adaptability to work with different types of boundary condition problems (Aichun et al. 2016). This method describes a boundary value problem governed by the Laplace equation in irrotational and potential flow:

$$\nabla^2 \phi = 0 \quad (4)$$

At the same time, these conditions have to be applied to the free surface (S_f), body surface (S_b), the bottom (S_0) and the surrounding surface at infinity (S_∞) (Beck 1994). For the wetted surface and the bottom, there is a kinematic condition:

$$\frac{d\phi}{dn} = V_B \cdot n \text{ on } S_B \quad (5)$$

$$\frac{d\phi}{dn} = V_0 \cdot n \text{ on } S_0 \quad (6)$$

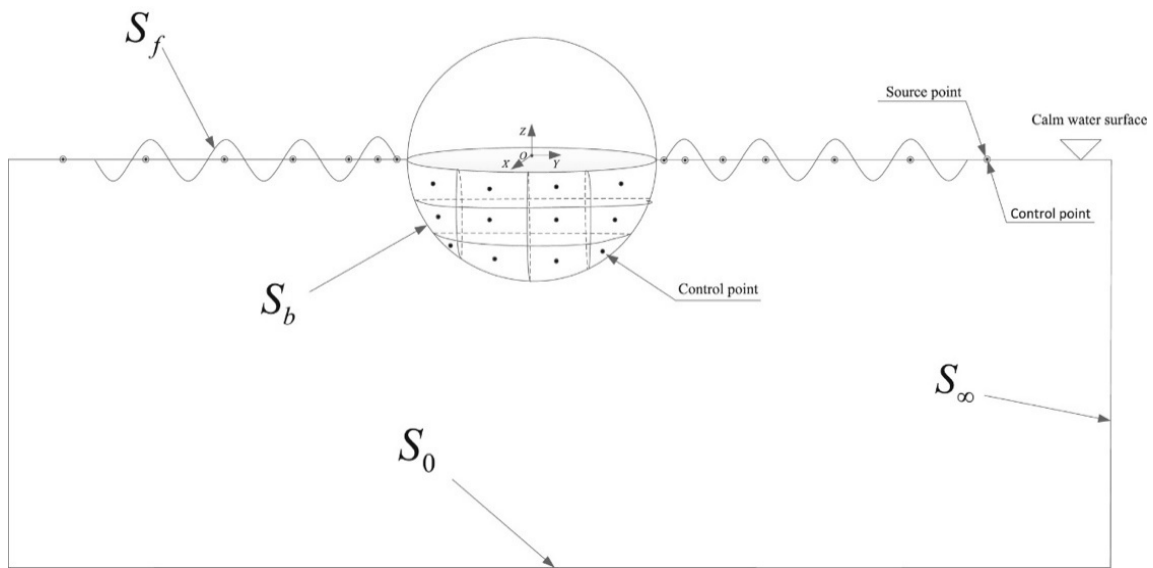


Table 4.1: Three-dimensional numerical model sketch (Aichun et al. 2016)

Where n is the normal vector, V_B is the velocity of a point in the surface and V_0 is the velocity of the bottom. For an infinite depth, V_0 will tend to zero. This way the all the fluid conditions interacting with the model can be described as it is seen in Figure 3.1. This gives two main advantages for the Rankine Panel method comparing it with other Panel methods such as the Green Panel method, these are:

1. Easy handling of the free surface conditions.
2. No use of irregular frequencies.

On the other hand, as a consequence of the problem description of the flow, the Rankine Panel method must consider the following boundary conditions (Bertram 2012):

1. There is no water flow considered along the ship surface.
2. Kutta conditions, the fluid pressure is the same at both sides of the edge of the hull.
3. Transom condition, the transom is considered to be dry.
4. Kinematic free surface condition, in the free surfaces there is no flow of water.
5. Dynamic free surface condition, the atmospheric pressure is considered in the free surface.
6. The effects of the ship on the water are neglected away from the ship analysis area.
7. Radiation conditions, the waves created by the ship disturbance move away from the ship.
8. Open boundary condition, the waves created leave the computational domain not returning after.
9. The forces on the ship produce ship motion.

4.2 Hydrodynamic interaction with the hull

The wave loads due to dynamic behavior are due to the difference between the forces of inertia and the forces due to hydrodynamic pressure on the hull surface (Fonseca and Guedes Soares 2004). This can be expressed as:

$$F_i(t) = I_i(t) - R_i(t) - D_i(t) - K_i(t) - H_i(t) - G_i(t) \quad (7)$$

$$M_j(t) = I_j(t) - R_j(t) - D_j(t) - K_j(t) - H_j(t) - G_j(t) \quad (8)$$

The subjects i j represents the associated ship motion to the different load components; being surge, sway and heave for forces and roll, pitch, and yaw for moments. The load components are the radiation (R) the diffraction (D), the Froude-Krylov force (K_k) and the restoring hydrostatic force (H_k).

For linear formulation in WASIM, the components for hydrostatic and Froude-Krylov forces calculated by the pressure integration of the mean wetted surface producing unrealistic distribution of stress in the splash zone, implying that the sea pressure above that value (Li et al. 2014).

The exciting forces due to the incident waves can be divided into two components: Froude-Krylov force and diffraction forces.

- **The diffraction force** is produced by the effect of the wave field while the vessel is moving. It is expressed as the advancement of the ship at a certain speed (considered constant for this thesis) while the ship goes through the waves and it is restrained by the mean position.
- **The Froude-Krylov force** is related to potential wave incident, is a result of the integration of the associated pressure over the hull wetted surface. In irregular waves, the wave field pressure is calculated through the harmonic superposition that defines the waves. As mentioned before, the linearity defines the wave pressure up to the mean of the waterline, thus making the hydrostatic pressure on the free surface negligible.

The hydrostatic forces are a result of the integration of the hydrostatic pressure on the wetted surface. For the linear method, this force is only computed under the undisturbed wave profile. In this case, the hydrostatic force components can be expressed as the standard linear of restoring force coefficients, as for heave and pitch (Singh and Sen 2007):

$$H_3 = \rho g A W P \xi_3 \quad (9)$$

$$H_5 = \rho g \nabla G M L \xi_5 \quad (10)$$

The radiation restoring force corresponds to the correction to the ship hydrodynamic forces due to the flow acting in the hull. The radiation force is related to that way to the restoring coefficients, being a collection of these with the memory functions representing the vessel properties moving at a certain speed.

The green water forces are the vertical forces related to the effect of green water on the deck. This one occurs when the relative motions are larger than the freeboard. The water force is proportional to the height of the water on the deck, which is the difference of the motions with the freeboard of the vessel.

4.3 Setup of numerical simulations

The numerical model of Stena Elektra has been designed by DNV GL for Chalmers following the hull design of Stena; this model has been specially designed for its use with the DNV GL SESAM software pack. The dimensions of the model follow the properties of the real size ship (Table 3.1).

The panel resolution of the model follows an aspect ratio of 0.03, which has been recommended by DNV GL. A convergence analysis has proven that this aspect ratio works for drafts between 6 and 7 meters. On the other hand, the use of a higher draft or ratio will degenerate into mesh errors.

The numerical simulation model is used to simulate the experiments presented in Table 3.4. To achieve that mass distribution, the simulated ship has to reproduce the experimental model geometric properties (See Figure 3.5). A calibration of the ship's weight is needed to reproduce as much as possible the same geometrical properties as the experimental model.

The computational methods need more detail and control in their calculations. Higher measurement and control of variables will help in the analysis against the model forces (ITTC 2011). For advanced numerical tools, motion control is needed as a requirement for an accurate prediction of ship motions (Lin et al. 2004).

A ship motion control has been set up in the simulation to keep the desired course of the model. These springs are attached to the bow and stern of the vessel to decouple the surge from saw and yaw (Figure 4.1). Both stiffness and damping are defined for the springs. In Wasim, the user does not specify the damping and stiffness coefficients directly. Damping is a fraction of the critical damping; that is why the stiffness is implicitly given by the specifying natural period in the modes control (DNV GL 2015b).

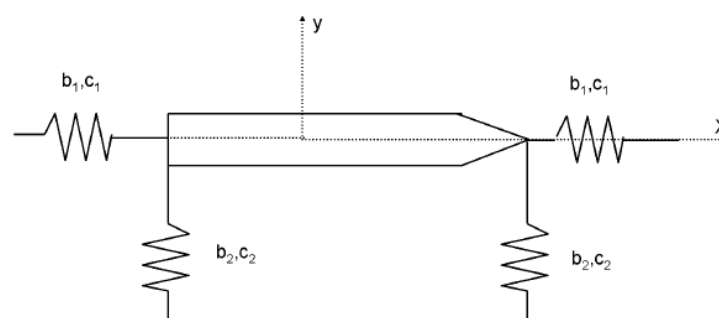


Figure 4.1: Motion spring in bow and stern (DNV GL 2015b)

The natural periods specified should be much longer than the natural period in roll in order to avoid interferences with the roll motion. Typical values range from 60-120s for conventional ships and 30-60s for high speed vessels. Notice that depending on the increase of this value may also affect the transient period of the simulation; the stiffness will be computed by assuming that the modes are uncoupled. Thus, the actual natural periods may differ from the periods given by the user (DNV 2006). These motion controls used in the simulation can be seen in Table 4.2.

Table 4.2: Motion control on the bow and stern

	Eigenperiods			Damping coefficients		
	Surge	Sway	Yaw	Surge	Sway	Yaw
For moderate speeds	100s	70s	70s	0.05	0.05	0.05
For high speed (21kts)	75s	45s	45s	0.45	0.45	0.45

To verify the hull structure of the numerical method, the eigenvalues of the numerical model will be analysed and compared with the experiment to ensure the behavior of the structure for hydro elastic behavior. This eigenfrequency analysis is carried out using the Wadam for floating and fix structures inside SESAM HydroD (DNV GL 2016) to find the resonance frequencies of the numerical model. This frequency is later compared with the results of the hammer test experiments.

Once the modal analysis has verified the model, the five different sea states are simulated using the Wasim code under the HydroD (DNV GL 2016). This software is meant for hydrodynamic analyses of fixed and floating vessels with or without forward speed, and at the same time, it also computes the motions and local pressure on the ship under study.

The conditions for the different sea states and seakeeping tests, shown before Table 3.4 and in Table 3.3, have been compiled in 16 different simulation runs to analyse. These are found in Table 4.3, where the relevant data describing each sea condition is found.

Table 4.3: Simulation conditions

Condition	Sea state	Speed (kts)	Wave direction (deg)	Significant wave height (m)	Wave period (s)	Relevant time for analysis [scaled] (s)
1	S004	15	180	1.88	7.56	681.939
2	S004	15	150	1.88	7.56	423.117
3	S004	18	180	1.88	7.56	552.437
4	S004	18	150	1.88	7.56	341.000
5	S004	21	180	1.88	7.56	115.000
6	S004	21	150	1.88	7.56	130.000
7	S005	18	180	1.88	4.00	200.000
8	S006	18	180	3.25	9.24	584.979
9	S006	18	150	3.25	9.24	340.148
10	S006	15	180	3.25	9.24	467.521
11	S006	15	150	3.25	9.24	441.122
12	S007	18	180	3.25	5.00	250.000
13	S008	12	180	5.00	10.78	980.116
14	S008	12	150	5.00	10.78	568.130
15	S008	15	180	5.00	10.78	475.307
16	S008	15	150	5.00	10.78	425.855

5 Results and discussion

The following chapter addresses the results of this thesis; a discussion of the assessment of the numerical results against the experimental data is also introduced. This chapter is divided into the calibration of the model, the frequency analysis and the different sections concerning the seakeeping simulations. The seakeeping simulations results are starts with the incident waves, and later the motions and loads are introduced.

5.1 Calibration of the numerical model

A series of masses were added in the experiment model that represented the ship in full load condition. These weights were distributed along the model resulting in the properties expressed in Figure 3.5. To reproduce those main characteristics, a calibration of the simulation model has been done using Sesam GeniE (DNV GL 2015a).

This calibration sets the mass points along the model, to represent the mass characteristics of the experiment, as well as the ones as in real scaled ship. For each segment, a mass point is added on the upper deck and in a lower deck aiming to reproduce the same VCG as well as the same LCG.



Figure 5.1: Numerical model analysis set up

The calibrated set-up of the mass points distributions of the model is presented in Figure 5.1 and Table 5.1. This distribution does not reproduce accurately the characteristics of each segment of the experimental model. Due that the mass point's distribution along the ship length does not follow the properties for their respective model segment. On the other hand, the calibration has achieved to reproduce the real size ship properties presented in Table 5.2.

Table 5.1: Mass component properties [kg]

	LCG=21.719m	LCG=75m	LCG=121m	LCG=166.463m
Upper deck (VCG= 5.40m)	1 089 915	1 202 709	1 246 946.56	667 056.44
Lower deck (VCG= 15.20m)	2 778 441	3 065 978	3 178 750.14	1 700 478.45
Hull weight [COG (87, 0, 8.121) m]	3 546 716.30			

Table 5.2: Numerical model properties

Weight [tones]	18 477
COG [m]	(88.895, -5.29e-06, 11.613)
Ixx [m ⁴]	6.469 e +008
Iyy [m ⁴]	4.5901e +010
Izz [m ⁴]	4.5682e +010

5.2 Frequency analysis

5.2.1 Hammer test

The ITTC recommended guidelines (Dinsenbacher et al. 2010) were used as the procedure to do the resonance test. Two hammer tests were carried out for dry and wet conditions to find the natural frequencies of the structure.

For the dry condition, the model was supported at two points at 1100 mm (or 40.7 meters scaled) from the fore and aft of the model as can be seen in Figure 5.2. A third support was placed in the middle of the model to avoid any big high motions on the structure. For the wet condition, the model was made to resonate in the wave basin supported only by the water in free vibration.

The results on dry conditions and wet conditions are presented in Table 5.1. While the impulsive excitation was applied, the bending moments and shear forces were recorded by measuring cells between the segment cuts. The Fourier spectrum and the bending moment throughout time graphs are presented in Figure 5.3 and Figure 5.4.

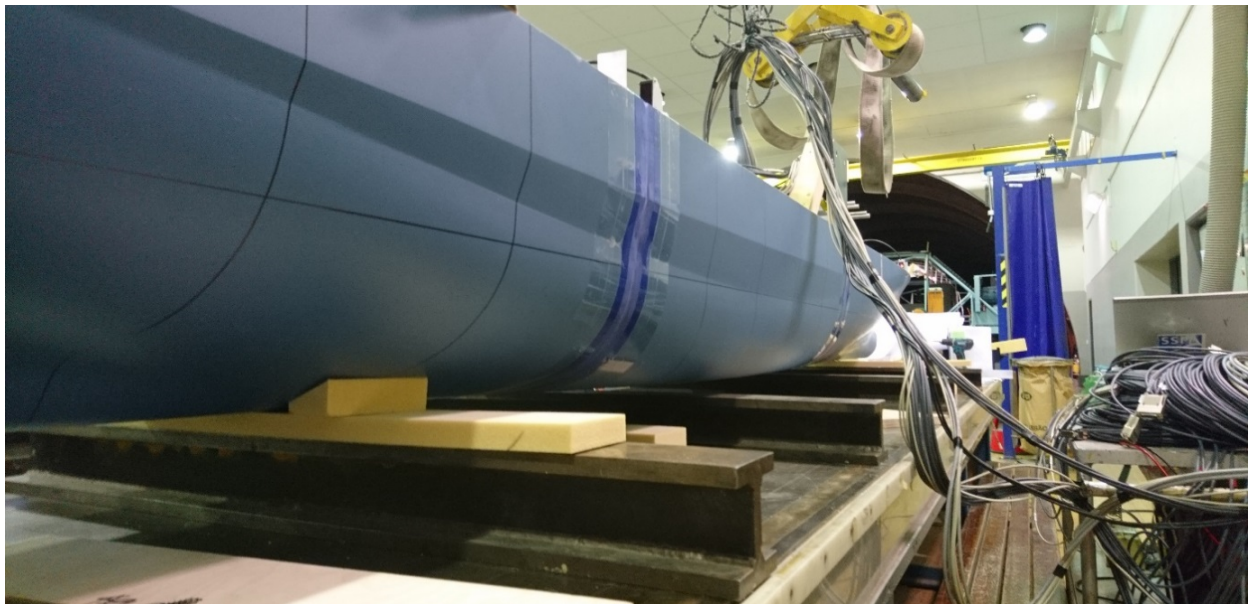


Figure 5.2: Picture of set up for resonance test

Table 5.1: Summary of results of resonance frequency test for two node bending

	Wet conditions		Dry conditions	
My/Cut	Resonance frequency model (Hz)	Resonance frequency full scale (Hz)	Resonance frequency model (Hz)	Resonance frequency full scale (Hz)
My/Aft	5.29	0.87	7.39	1.22
My/Mid	5.29	0.87	7.39	1.22
My/Fore	5.29	0.87	7.39	1.22

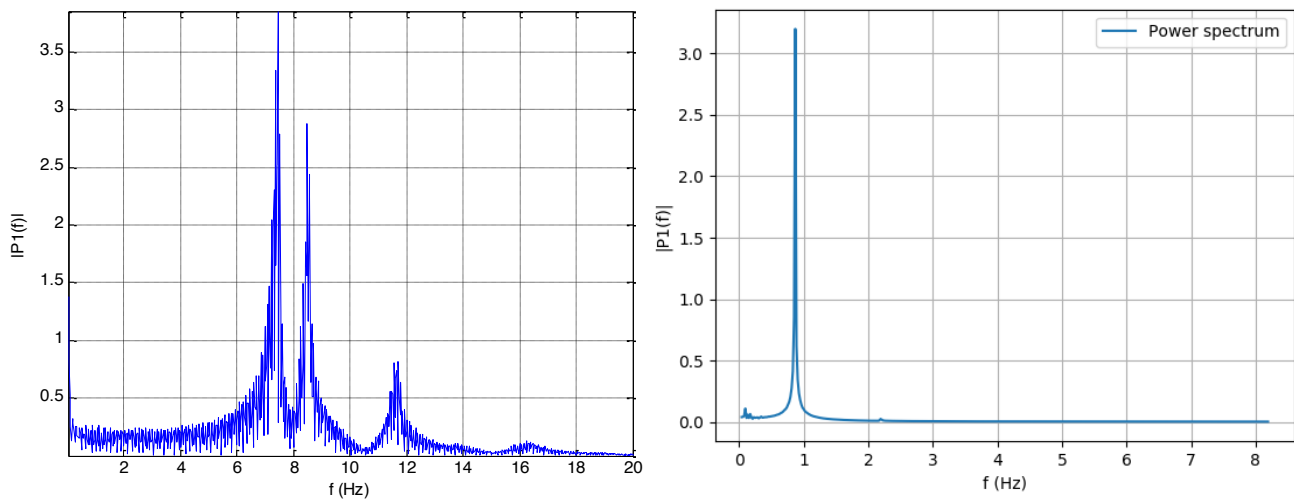


Figure 5.3: Single sided Fourier spectrum of bending moment at mid cut for (left) wet and (right) dry test conditions

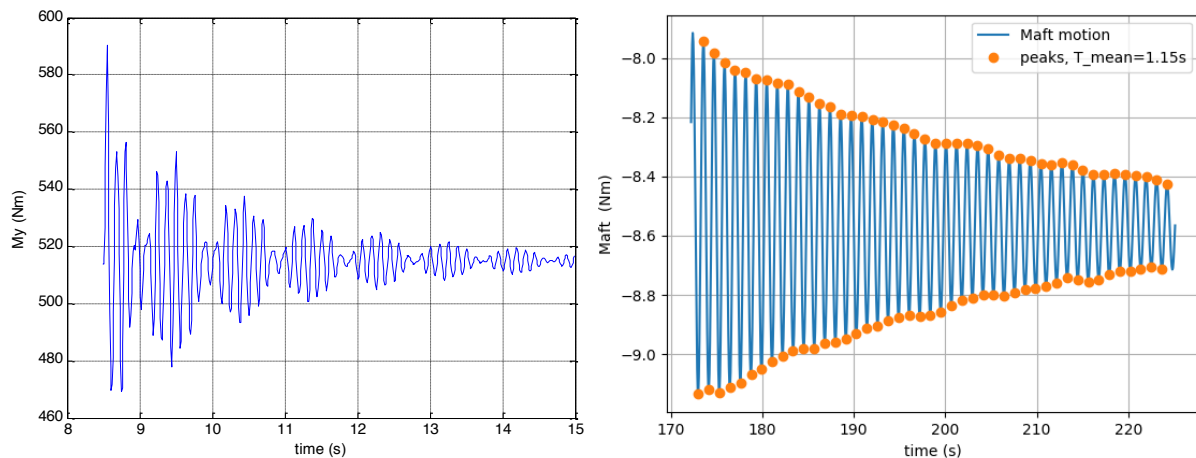


Figure 5.4: Time history of bending moment at mid cut for (left) dry and (right) wet test conditions

5.2.2 Eigenfrequency analysis

The numerical eigenvalue analysis set-up simulates the mass distribution of the model (Figure 3.5). This distribution is reproduced in the FE model in GeniE (DNV GL 2015a) as it has been presented in Section 5.1.

The eigenfrequency analysis for wet conditions has been simulated with the Wadam code inside HydroD (DNV GL 2016). Wadam is an analysis program for the computation of wave-structure interaction for fixed and floating structures. The Wadam code allows to extract the natural frequency from the wet condition in free vibration for a rigid body motion.

The result extracted from the code gave 0.79 Hz as the natural frequency of the model, showing a good performance in the model calibration with a difference of 9.1%. As expected, the numerical eigenfrequency is lower than the one the hammer test, showing the apparent effect of the rigid body. Under vibration, the behavior of the segmented model in the water environment affects each one of the segments producing a higher frequency reading.

The discrete mass distribution presented in Section 5.1, proves to be an effective and practical simplification to the real distribution in the experiment. A better mass distribution as well could improve the result obtained. Another cause of deviation for the simulation is the rigidity of the numerical model. Other factors due to the uncertainties of the experiment could have also affected the divergence of results.

For the calculation of the dry condition, the eigenfrequency has been computed with the GeniE (DNV GL 2015a) under its Sestra code. For the computation of the eigenanalysis, Sestra treats the model as a beam making it dependent on the geometry, mass distribution and supports, as boundary conditions. The treatment of the numerical model as a beam is a cause of uncertainty in the calculation as it does not allow a free vibration analysis.

For the frequency analysis, two support arrangements in the analysis setup are presented; their configuration is in Table 5.2 and Figure 5.5 and Figure 5.6. The first one introduces the supports at the edges of the model aiming to reproduce the vibration of the whole vessel fixed in the edges, giving a resultant frequency of 0.33 Hz for the first vertical mode. The second configuration aimed to reproduce the behavior of the hammer test experiment having the supports at 40.7 meters from aft and fore resulting in 0.72 Hz.

Table 5.2: Boundary condition of the supports

Arrangement		Position [m]	x	y	z	rx	ry	rz
1	Support 1	(-4.5, 0, 7.4)	free	fixed	fixed	free	free	free
	Support 2	(195.5, 0, 7.3)	free	free	fixed	free	free	free
2	Support 1	(36, 0, 0)	fixed	fixed	fixed	free	free	free
	Support 2	(154.4, 0, 0)	free	fixed	fixed	free	free	free

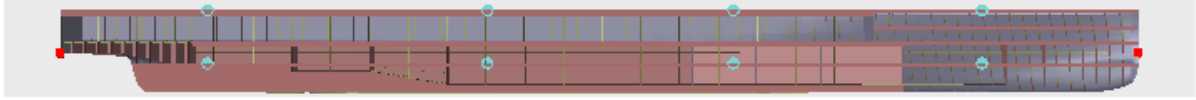


Figure 5.5: Dry eigenanalysis arrangement for layout 1

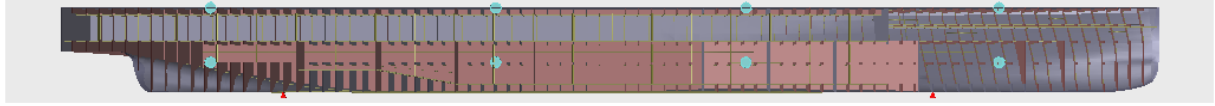


Figure 5.6: Dry eigenanalysis arrangement for layout 2

Due to the large difference of results with the hammer test (1.22 Hz), none of the simulations performed are satisfactory in the dry vibration analysis. Uncertainties on the setup or in the treatment as a supported beam by code could be a reason for these results. A problem in the nature of the rigid body against the segmented model could be a reason for some discrepancies in the vibration, but due to the high difference presented, this option is disregarded. Other factors that could also affect the computation could be the size of the numerical model, but it is unlikely due to the nature of the software. In the end, the numerical simulations failed to provide a valid result in water conditions.

To provide a more representative result in the dry condition analysis, the Immersed beam formula is introduced (Equation 12). This approximation work on the assumption that the fluid where the beam is immersed is incompressible (Sader 1998), assumption already been made by the panel method, see Section 4.1.

For a dry environment, the eigenfrequencies have been overestimated by the numerical results, inconsistencies that are uncertain for the conditions of this analysis. This divergence in the results could be due to the misuse of the software properties in frequency analysis. For that, the use of an approximation is introduced for the assessment of this value. This consist of

$$w_{fluid} = \frac{w_{vacuum}}{\sqrt{1 + \frac{\pi b \rho_{fluid}}{4 h \rho_{beam}} \Gamma}} \quad (12)$$

where (Veryst Engineering 2019):

- 1) Γ : is the correction factor dependent on the geometry of the beam.
- 2) ρ_{fluid}/ρ_{beam} : is the density ratio
- 3) b is the aspect ratio

For practical use in water, the equation can be summarized in the following:

$$\frac{w_{air}}{\sqrt{2}} = 1.015w_{water} \approx w_{water} \text{ (1\% or 2\% deviation)} \quad (13)$$

This simplified version of the immersed beam vibration formula (Equation 13) that has been proven to work correctly in the correlation with the experimental results. The formula used comes from its extended version in Equation 12, where the value of the coefficient for the different frequencies are the result of the properties of the ship cross-section and environment conditions.

The calculated results presented show a slightly similar results with a natural frequency of 1.13 Hz in dry conditions and an error of 7.3% from the experimental test. The resultant frequency of the analysis can be found in Table 5.3. Hence, under these circumstances, the agreement between the experimental and the numerical model is considered to be satisfactory.

Table 5.3: Results eigenfrequency analysis

	Numerical [Hz]	Experimental [Hz]	Difference
Wet condition (simulated)	0.79	0.87	9.1%
Dry condition (approximation)	1.13	1.22	7.3%

5.3 Seakeeping simulations

A total of 16 seakeeping simulations have been carried out following the properties of Table 4.3. These simulations done in HydroD (DNV GL 2016) follow the weight distribution presented in this work as well as the main conditions expressed in Section 4.3.

For the seakeeping test carried in SSPAs MDL wave tank, a draft of 6.3 meters was fixed for all simulations to reproduce the desired draft desired behavior of Stena’s design. An offset on the seakeeping experiments has been found as a result of that draft. To simulate it, in the seakeeping simulation, the draft has also been fixed at 6.3 meters.

The simulations are carried out with the JONSWAP spectrum to define the wave profile. The simulation follows the linear wave theory with irregular waves. A standard of 2000 wave components have been selected for each simulation. The time for each simulation is of 30 min (1800sec) with time steps of 0.1 sec, a transient period of 100 sec for each simulation has been selected in order to produce a smoother transition at the start of the simulation.

The simulations have been carried out on time domain in Wasim and later analysed against the scaled experimental data in MATLAB (Mathworks 2016). The statistical analysis and conversion to the encounter spectrum are done using the WAFO toolbox (Brodtkorb et al. 2000). The main particulars for each simulation can be found in the appendix.

The sea motions of the numerical simulation have been recorded accordantly to the experimental model. For the simulation, the motions are measured in the midsection at draft height. The motion simulated follows the control spring motion presented in Section 4.3. The cross-section loads are measured in the aft, mid and fore section of the model.

5.3.1 Incident waves

The incident wave height has been analysed in order to ensure a good estimation of the wave impact on the model. This estimation has been done by setting the incident wave height on the time domain in the spectra. This way a good fit of the incidental wave will ensure the quality of the incident irregular waves (Zhu et al. 2011a). A display of the wave spectra for different simulation conditions is shown in Figure 5.7. Where it can be observed that both results show a good definition of the JONSWAP spectra profile. In calmer sea states at low speed the incident waves of experiment and simulation stay similar; at lower speeds the incident of waves on the hull decreases. As the sea state becomes higher the numerical incident wave surpasses the experimental prediction. This could be due to the linearity of the waves and its assumption of not considering the wave effect of the water flowing thorough the hull. The linearity of the numerical result is also compromised at high-speed such as it can be seen in S004. There, the spectrum starts to overestimate the experimental result.

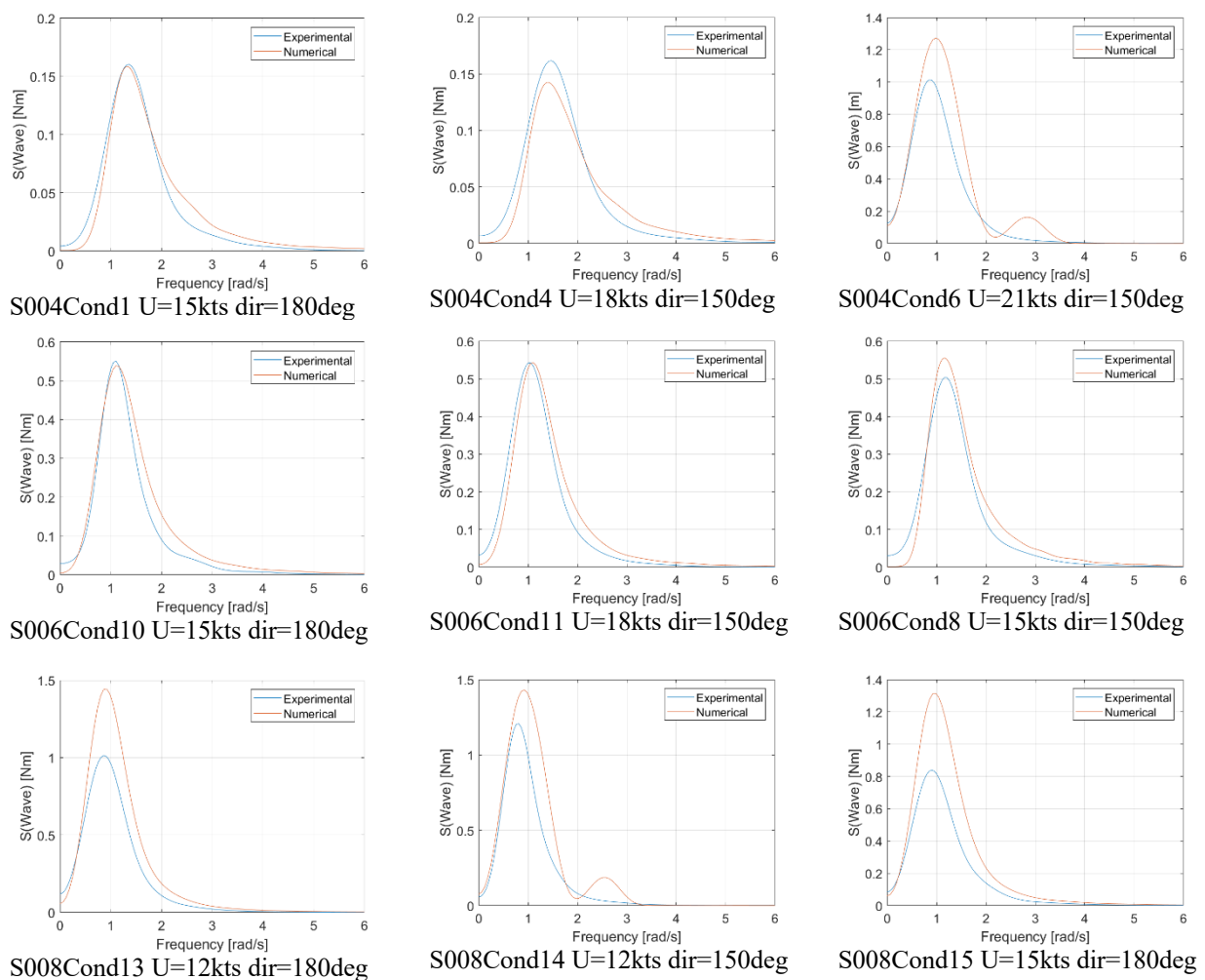


Figure 5.7: Incident wave spectra for the three non-crested sea states for different heading angle and speed.

In short crested waves, the spectra show more discrepancies than the other sea states between the experiment and the simulation. Even if the energy spectra are similar, the fact that the peak

of the numerical spectrum is found at a higher frequency is indicative of greater discrepancies in the other motions.

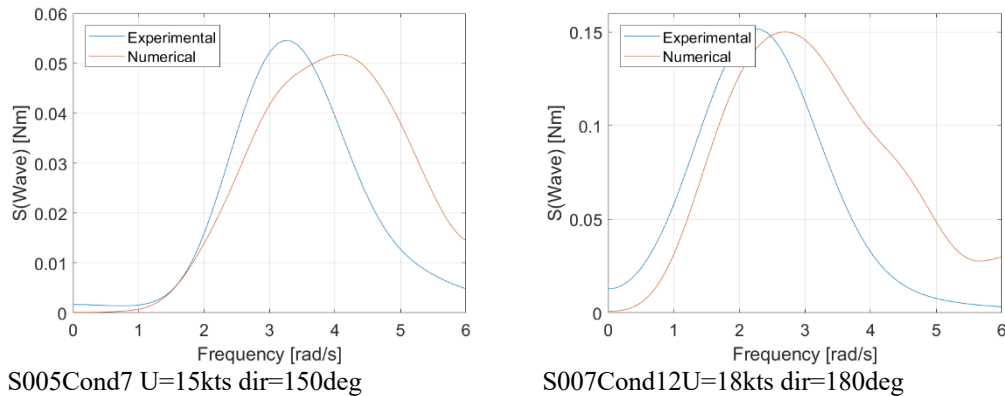


Figure 5.8: Incident wave spectra for short crested sea states

These performances of waves are indicative of the simulation set for the wave grid, as well as how the motions and loads will be predicted in the different conditions. Even though the area beneath the graph shows that the simulations have higher wave energy, they are still similar. At the same time, the spectrum peak of the numerical simulation is set at a higher frequency. Nevertheless, it can be said that the definition of JONSWAP waves in the simulations achieves to give an accurate description of the sea states, especially in lower seas.

5.3.2 Heave motions

All the global motions responses have been measured at the mid-section at draft height. In the motion analysis for heave, the overall results seem to be accurate. The major divergences are found as the sea states become higher. It is observed that the heave values do not move around zero, even in the lower sea state conditions. For a consequence of the draft offset in the setup of the seakeeping tests for both experiment and simulation.

In Figure 5.9, different seas states at the same speed are showcased. From there the peak values for heave in the simulations shown in the time domain are higher than the experimental ones. At the same time, the standard deviation is also higher in the numerical simulation increasing with each sea state, and this is clearly shown on S008Cond13. As the sea state becomes higher, the amplitude of the numerical result increases showing a more uniform response than in the experiment test. These effects can also be seen in the spectrum where the numerical responses show higher energy.

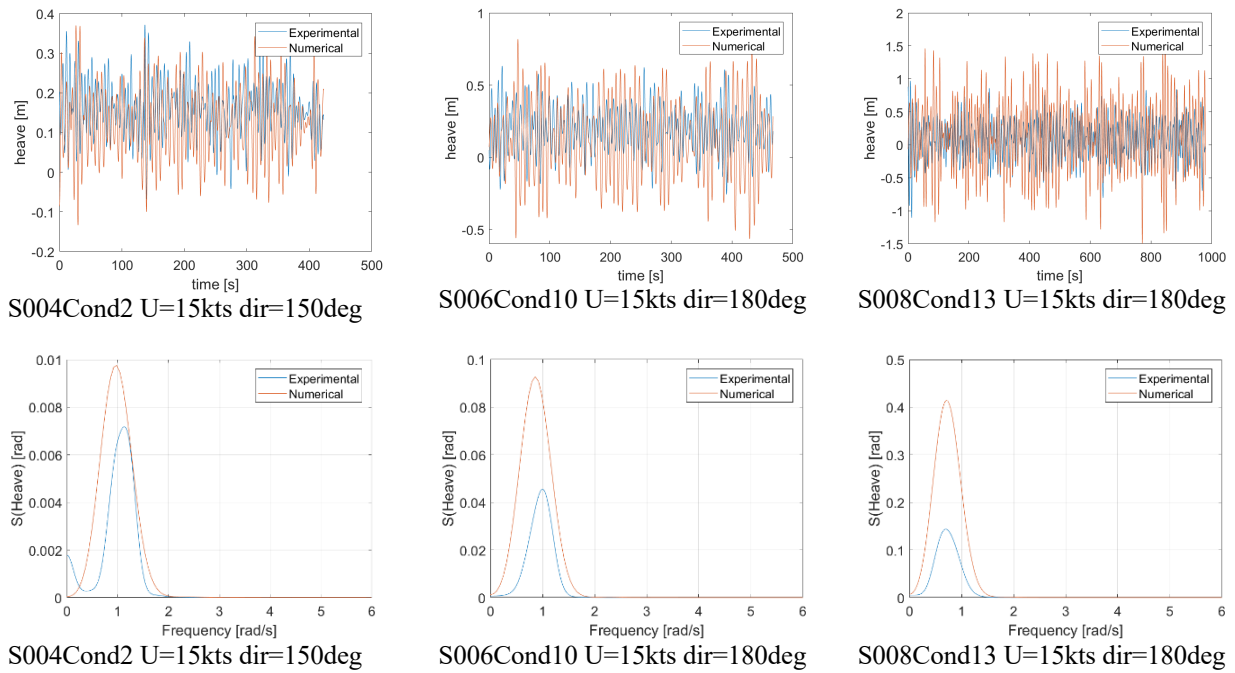


Figure 5.9: Heave motion in the time domain for non-crested seas

At lower speed, the heave mean value of the experiment and simulations remains very similar, with a mean difference of 13% between each other. This difference increases with the ship speed, showing a clear difference at high speeds, the simulated mean value is at 0.12m against the 0.26m of the experimental. The standard deviation does not vary a lot with the speed showing similar patterns between numerical and experimental. This can be seen in similarities of the spectrum for the three speeds, as shown in Figure 5.10.

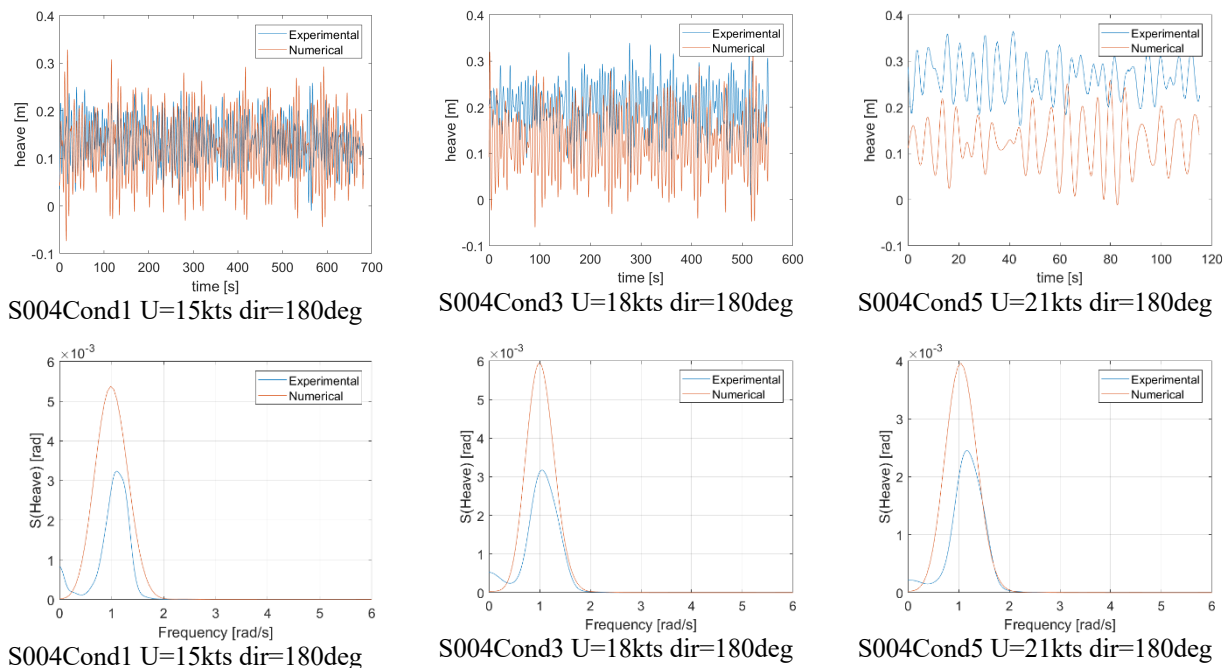


Figure 5.10: Heave response in S004 for different speeds

5.3.3 Pitch motions

The resulting pitch motions present similar differences with the heave responses between experimental and numerical tests. The numerical standard deviation is larger than the one in the experiments; this difference increases with the vessel speed. These results in an overestimation of the spectra energy in by the simulation as it is shown in Figure 5.12.

The increase of the sea state does not particularly affect much in the accuracy of the result were in differences between the most sea states stay similar, as it can be seen in S004 and S006 where the standard deviation differences with the experiment is around a 95%.

On the other hand, some inconsistencies are shown in the short-crested seas predictions, especially concerning the difference of the mean value, as it is shown in S007Cond12. This effect is slightly higher in the experiment, producing that the peak in the spectra is at a lower spectrum frequency.

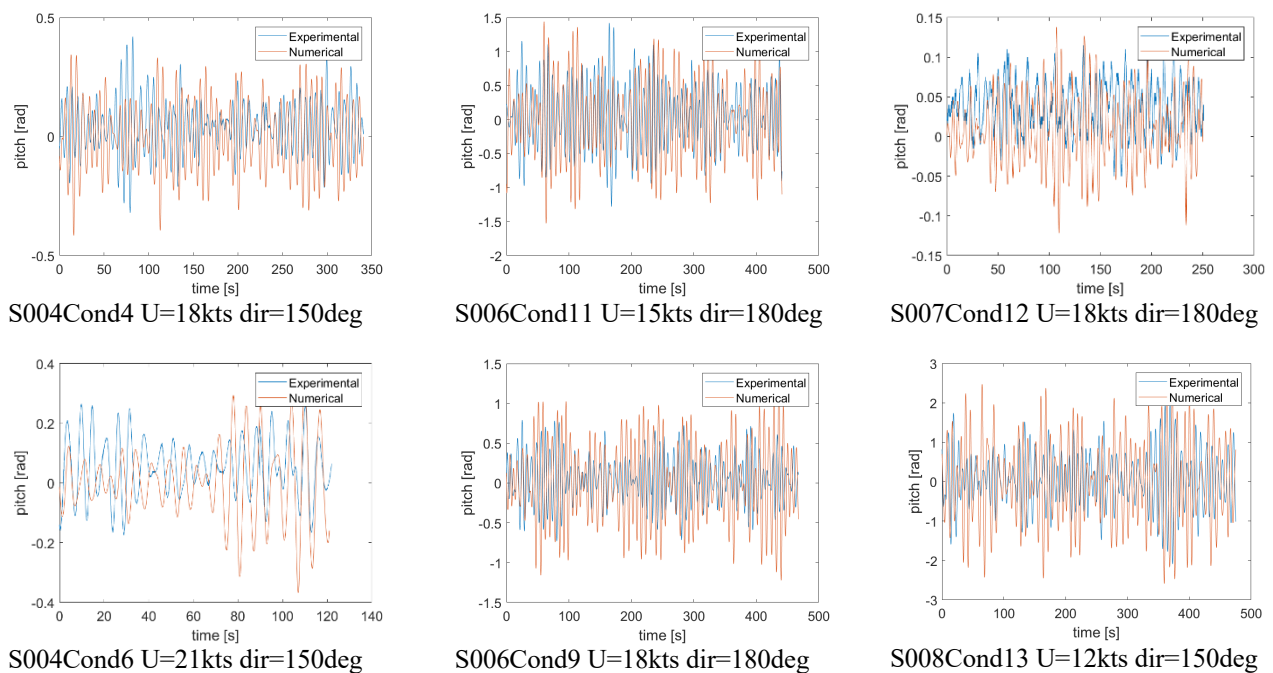


Figure 5.11: Pitch response in time domain

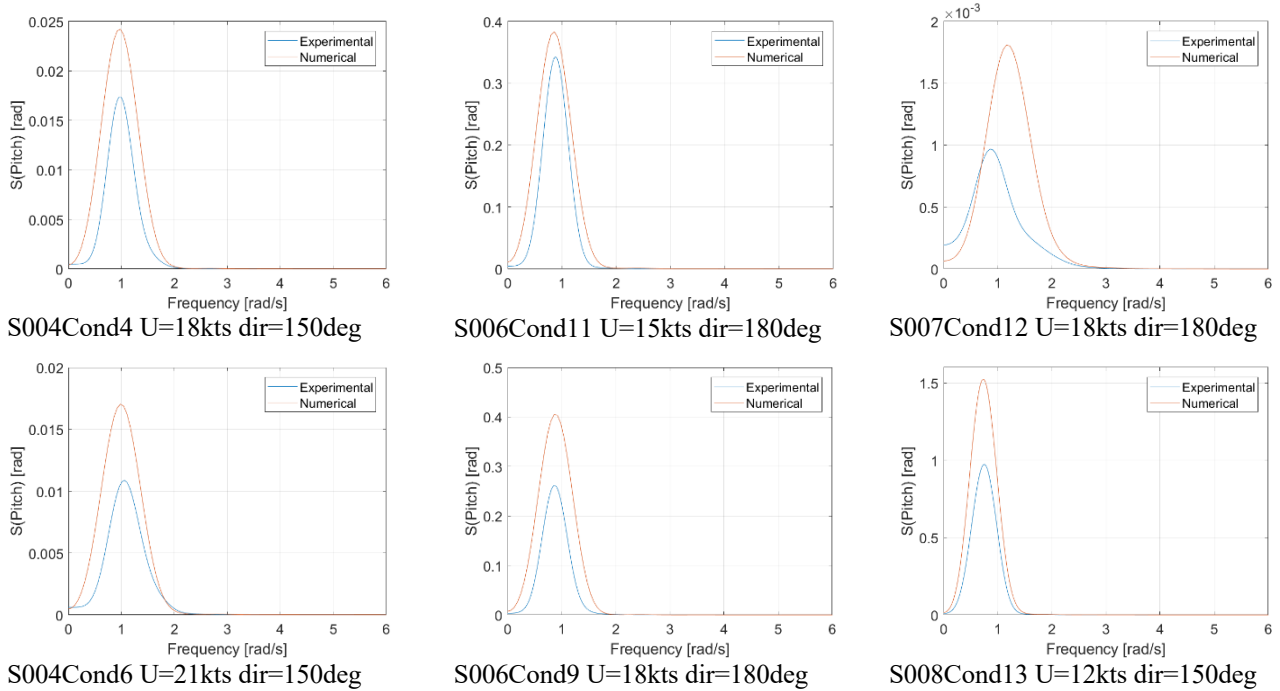


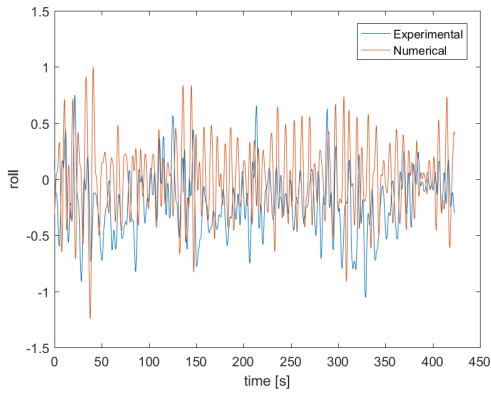
Figure 5.12: Pitch response in the spectrum

5.3.4 Roll motions

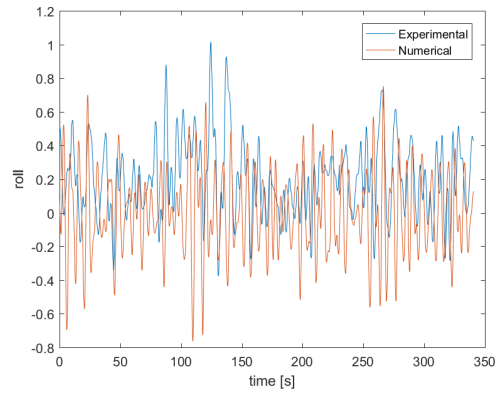
The roll motion for oblique seas is also presented in Figure 5.13, showing similarities in the motion response. The numerical values move through similar mean values. The standard deviation of the numerical motion on time domain surpasses the one in the experiments as the sea state changes.

These divergences due to the absence of roll damping in the numerical simulations. The roll damping is a resultant of the decrease of the roll angle amplitude due to the loss of energy. In this case, the roll damping is mainly produced by the viscous friction and the wave radiation, effects in which due to the simulation set up (concerning with the Rankine panel method) have been neglected.

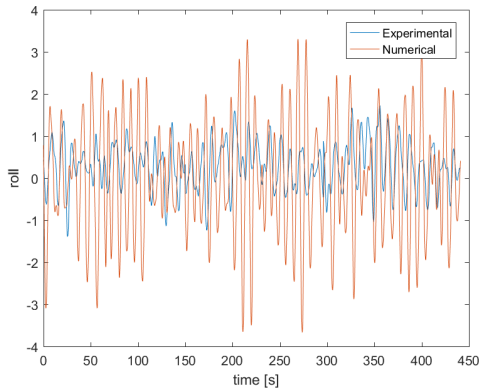
Another factor to consider is the scatter of the experimental data. On the other hand, the numerical result can be divided into sections; the values along the time domain follow a more predictable pattern. In this case, the rigidity of the numerical model could be a reason for this predictable trend. However, a more flexible experimental model could have had an unpredictable motion response by the waves affecting individually each one of the segments.



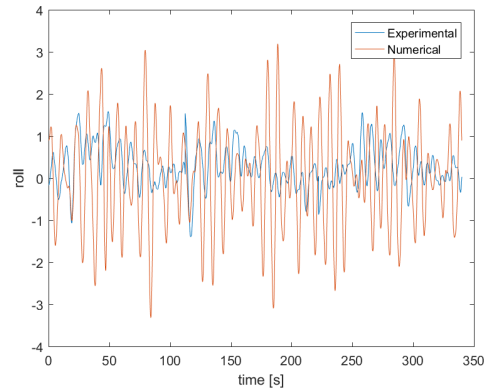
S004Cond2 U=15kts dir=150deg



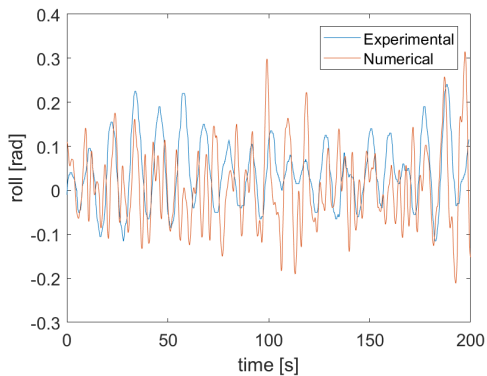
S004Cond4 U=18kts dir=150deg



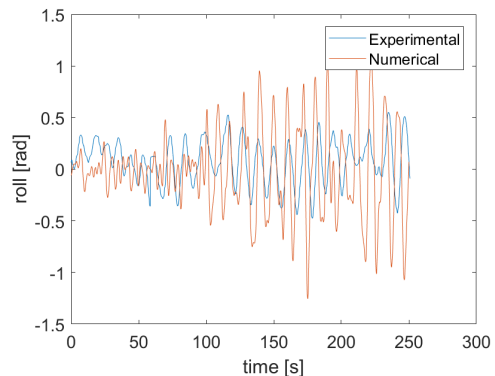
S006Cond11 U=15kts dir=180deg



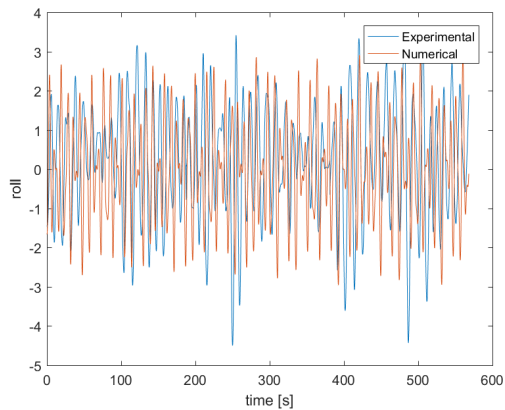
S006Cond9 U=18kts dir=150deg



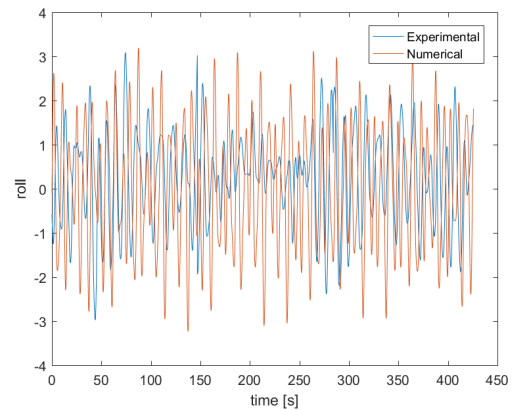
S005Cond7 U=15kts dir=180deg



S007Cond12 U=18kts dir=180deg



S008Cond14 U=12kts dir=150deg



S008Cond16 U=15kts dir=150deg

Figure 5.13: Roll motion in time domain

5.3.5 Shear forces

The cross-section shear force at the midsection for the different sea states is also evaluated, the results in spectra and time domain can be seen in Figure 5.14 and Figure 5.15. The negative values of the shear force on the mid-section indicates that both models are under a sagging condition.

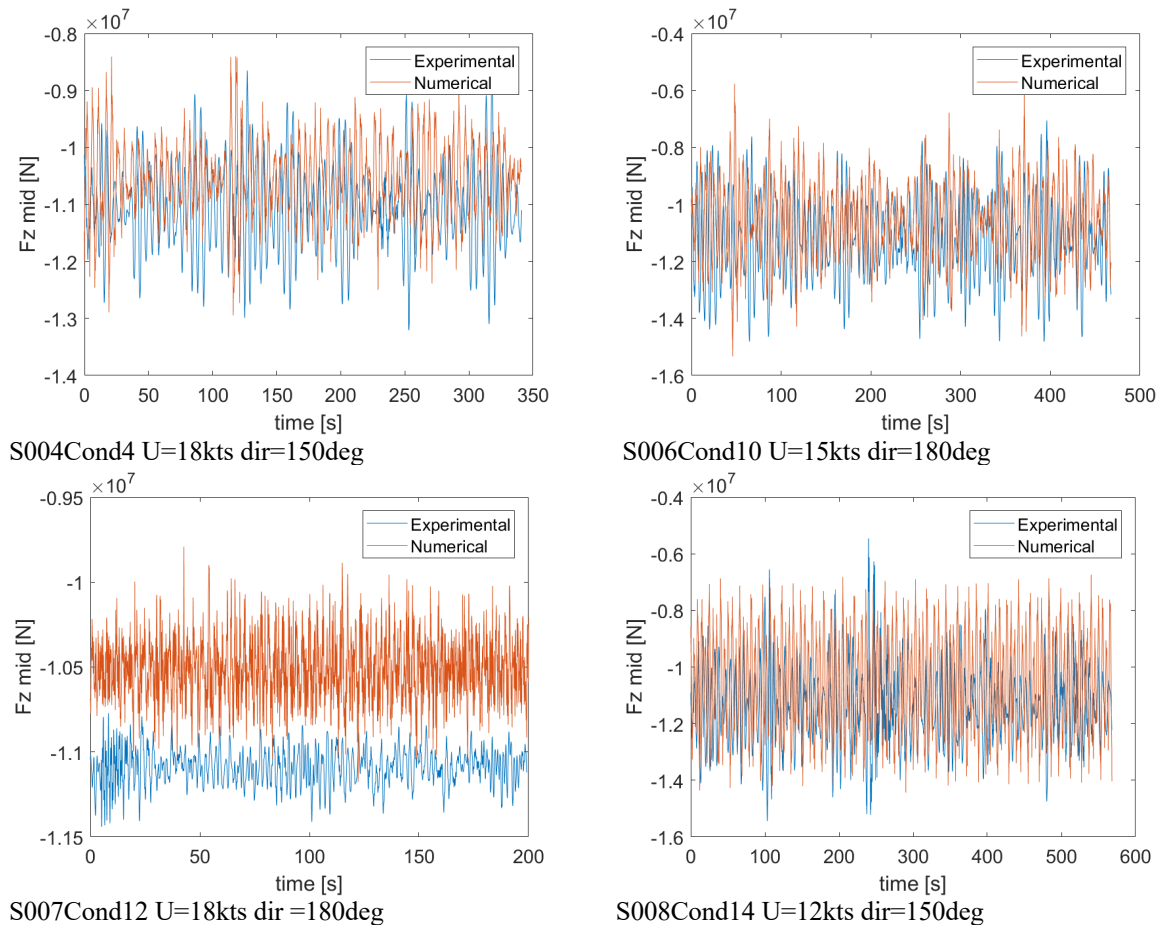


Figure 5.14: Shear forces for mid-section in the time domain

Due to the rigidity of the model and the use of linear wave theory, the simulated shear forces show symmetries around the mean value in all sea states; these are shown as the waves become higher as in S008. On the other hand, in the experimental reading there is no that much symmetry as in the simulation. Even in the calm S004, where there are should not be nonlinearities, a less predictable trend is seen, where the experimental peaks exceed the numerical results. An explanation for this could be the wave load effect on each segment of the experimental model. The freedom of each segment to respond individually to the vertical wave loads in the much more flexible experimental model results in a less stable reading of data, in contrast with the rigid model used in the simulations.

The numerical model proves to capture accurately the shear force behavior in terms of mean values where the difference for all sea states is within 7% of the experimental model. These relatively small differences in the mean value could be due to different factors. There is a

possibility that there are some discrepancies due to scaling and model geometry on the measurement cross-section from both models. Differences due to draft position could cause a difference in the mean value of the force.

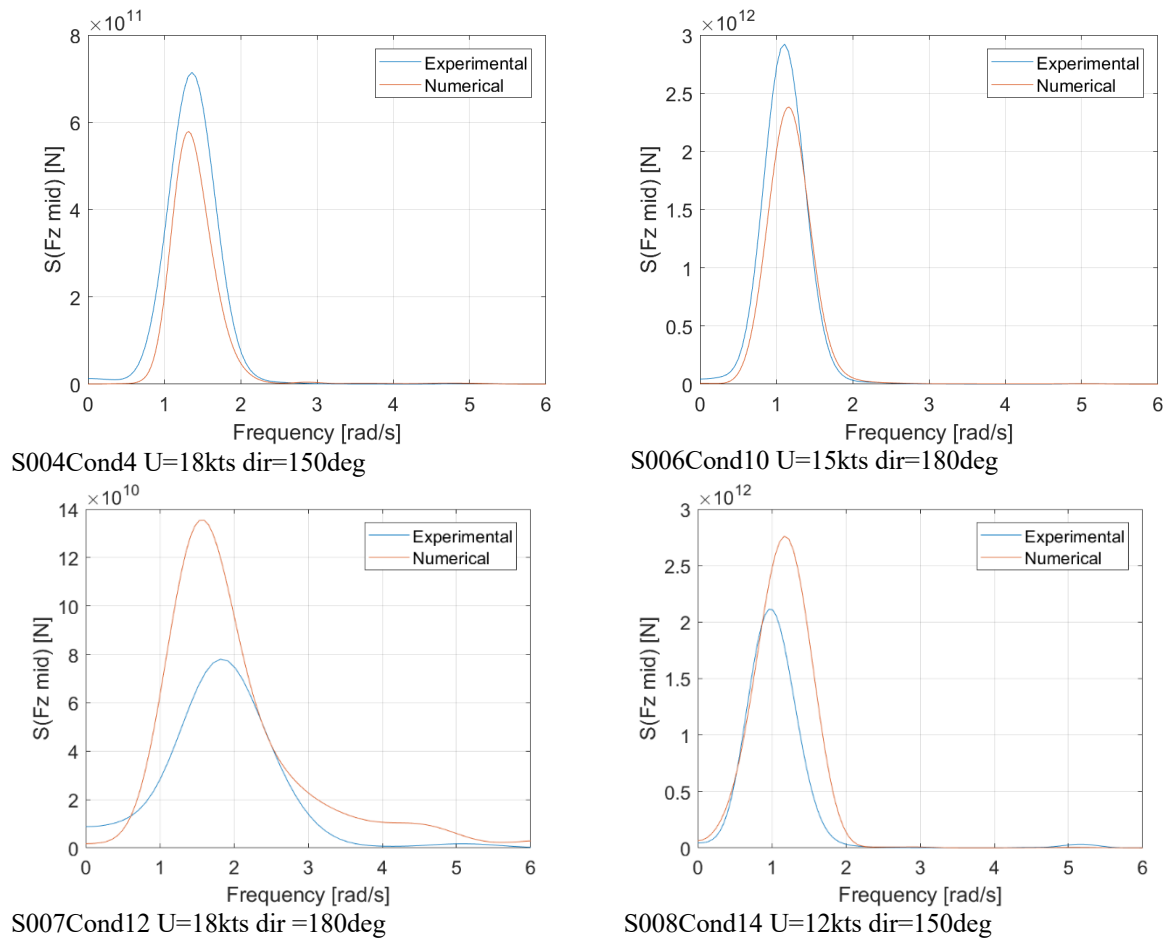


Figure 5.15: Shear forces for mid-section in frequency domain

At the same time, the standard deviation stays within an error of around 20% of the model test. In S007 the small shear force amplitude of short crested seas causes the numerical result not overlapping the experimental data. By S008 the numerical amplitude overestimates the experimental shear values presenting a very uniform trend and showing that the rigidity of the numerical model compromises the accuracy of the prediction. Other factors affecting the results are due to the nonlinear effects of the sea state being introduced into the experiment in the wave basin as the sea state gets higher.

The vessel speed also affects the shear force; as the speed increases the load does the same. This increase of the shear force becomes underestimated by the numerical simulations as the ship speed increases as can be seen in Figure 5.16. The increased speed affects the accuracy of mean values producing an underestimation of its prediction. At the same time with the speed increase, an underestimation of the standard deviation also occurs, as is seen in S004Cond5.

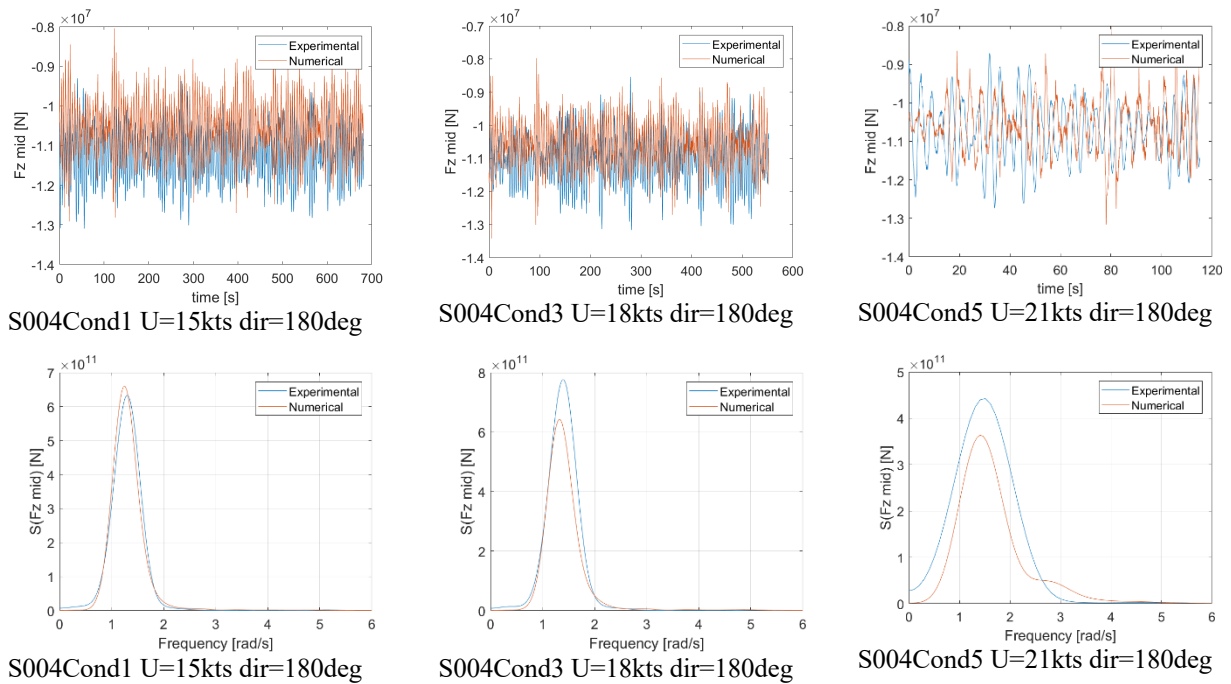


Figure 5.16: Shear force through different speeds

From a general perspective, the numerical prediction of the shear forces is accurate due to the differences in mean and standard deviation between models, shown in Table 5.4. It is clearly stated that two main parameters are the ones affecting the accuracy of the prediction: the increase of sea state and the increase of speed. It is on the combination of these two factors where the numerical prediction starts to be compromised (as seen in S007Cond12). On S008, we see that even with the high seas, the prediction is not compromised due to low and moderate speeds used there.

Table 5.4: Mean and standard deviation numerical difference of the experimental data for Shear forces

Fz	Mid	Mean error	Standard deviation error
S004	Cond1	0%	0%
S004	Cond2	-6%	-21%
S004	Cond3	-5%	-9%
S004	Cond4	-5%	-16%
S004	Cond5	-2%	-15%
S004	Cond6	-5%	-16%
S005	Cond7	-5%	-12%
S006	Cond8	-5%	-15%
S006	Cond9	-4%	-7%
S006	Cond10	-6%	-9%
S006	Cond11	-6%	-11%
S007	Cond12	-5%	36%
S008	Cond13	-7%	2%
S008	Cond14	-7%	23%
S008	Cond15	-6%	16%
S008	Cond16	-6%	17%

5.3.6 Vertical bending moments

The vertical bending moments at the midsection for the different sea states are presented in Figure 5.17 for the time domain and in Figure 5.18 for the frequency domain. The numerical vertical bending moments follow a good relation with the experimental model.

From the time domain result, the numerical moments show higher peaks in most of the sea states. Similarly, the shear forces both models follow a steady symmetry around their respective mean values, showing great similarities in the prediction. This symmetry starts to be compromised with the vessel at higher speeds and in higher sea states, where some wave linearity starts to be introduced.

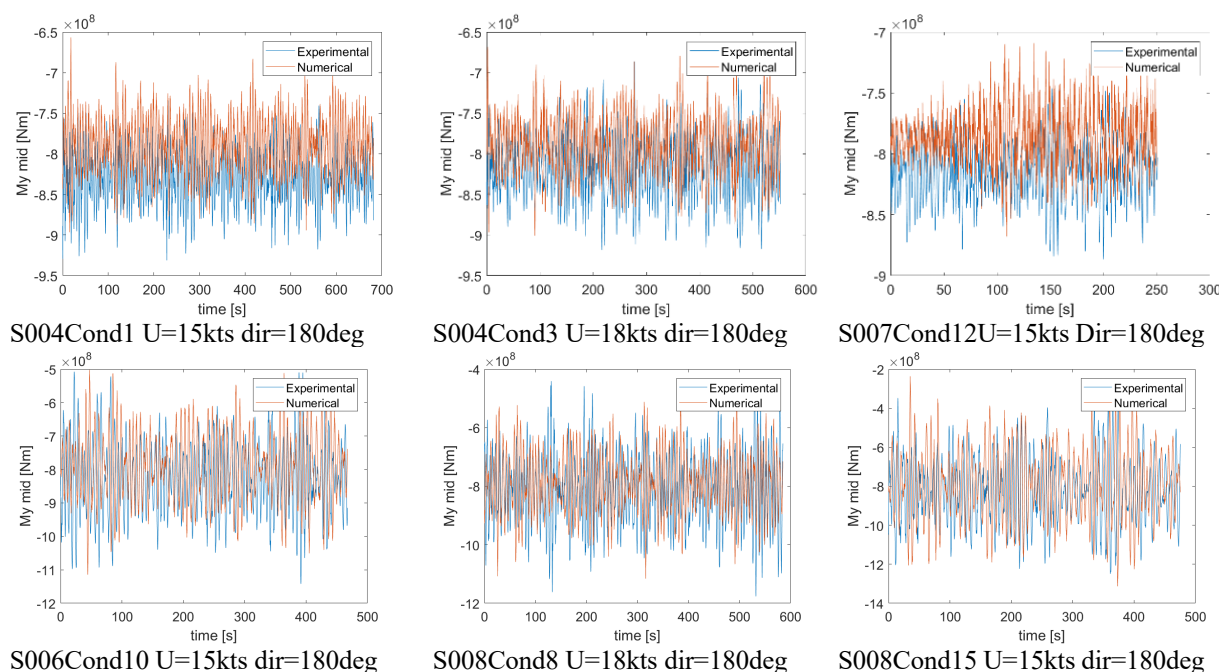


Figure 5.17: Vertical bending moment for Mid-section in time domain

The frequency domain graphs also show good agreements with the experimental results; the spectra area also shows agreements, showing similarities between both models. In Table 5.5, the difference from the experimental bending moments are showed cased. The nonlinearities do not seem to dramatically affect the predictions showing small differences in standard deviation. However, some indication can start to be seen at the higher sea states as well as at high speeds. It can be said that the simulation is able to predict accurately the segmented model behavior for all sea states.

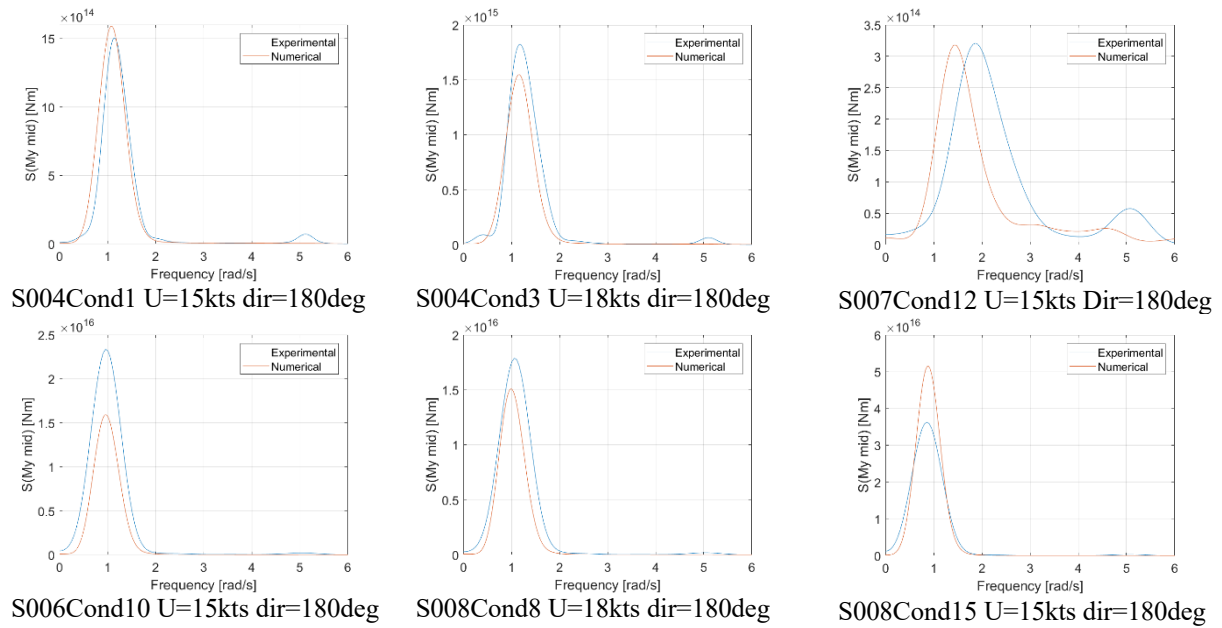


Figure 5.18: Vertical bending moment for Mid-section in frequency domain for heading seas

Table 5.5: Mean and standard deviation numerical difference of the experimental data for Vertical Bending moment

My	Mid	Mean error	Standard deviation error
S004	Cond1	0%	2%
S004	Cond2	-5%	-18%
S004	Cond3	-3%	-9%
S004	Cond4	-3%	-20%
S004	Cond5	-1%	-11%
S004	Cond6	-3%	-20%
S005	Cond7	-4%	-8%
S006	Cond8	-3%	-17%
S006	Cond9	-3%	-14%
S006	Cond10	-4%	-7%
S006	Cond11	-5%	-25%
S007	Cond12	-4%	6%
S008	Cond13	-5%	-7%
S008	Cond14	-5%	-3%
S008	Cond15	-4%	6%
S008	Cond16	-3%	-7%

5.3.7 Torsional bending moments

The simulated torsional bending moments on oblique seas are shown in Figure 5.19 with the experimental data. As expected, the numerical torsional results show wide discrepancies due to the rigid nature of the numerical model. Usually, the use of experimental model tests is more suited for torsion providing more detail readings, against the numerical prediction that are usually more focused on vertical prediction (Zhu et al. 2011b).

This is seen in the results presented where, due to the nature of the models, the results do not show the same symmetric behavior as in the previous vertical moment. The experimental

maximum and minimum peaks are higher, nearly all sea states. The more scatter behavior of the experimental data due to the flexible behavior of the segments is seen in all sea states, being especially pronounced on S008Cond16 against the linear numerical trend. At this high sea states, the numerical symmetry of the moments, show larger discrepancies between the models' rigidity.

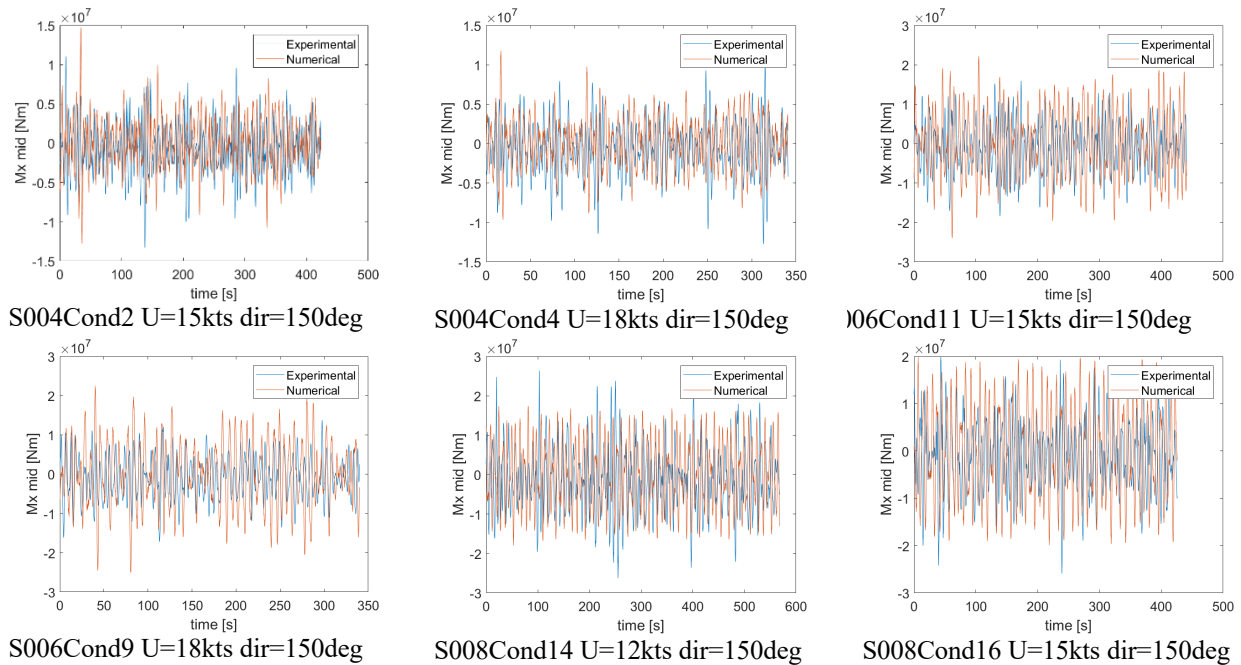


Figure 5.19: Torsional bending moment in mid-section for oblique seas

The spectra show the effect of the speed vessel in the prediction accuracy. There is an overestimation of the numerical simulations as the speed. On the other hand, in the lowest sea state, the numerical accuracy is high, showing agreements in the spectrum.

As an overall view of the torsional moment results, the numerical values cannot be used as an adequate prediction of the experimental behavior. A numerical difference in mean values of around 100% is in all sea states. This difference could be due to geometric and scaling uncertainties, but they cannot be taken as proper reference. It is only in the standard deviation results cases as in the lowest sea state S004 and in slowest speed S008Cond14 where there is some accuracy of the simulation. In these, the numerical model could be used as a reference to understand the magnitude of the motion.

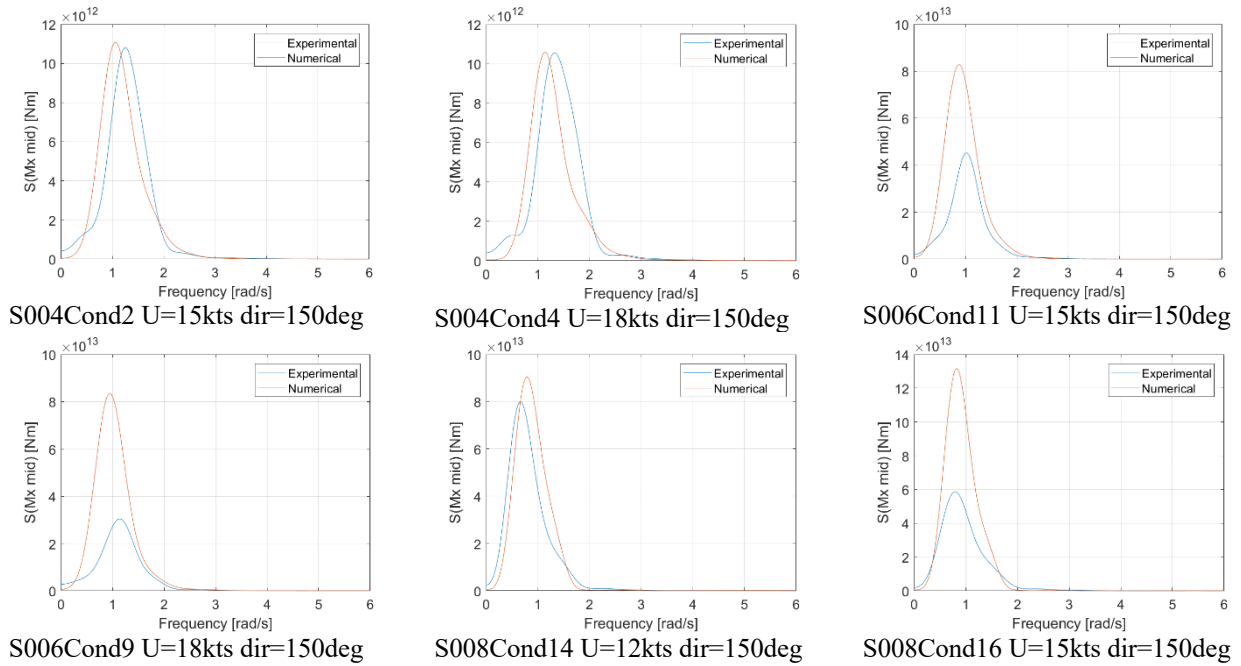


Figure 5.20: Torsional bending moment in mid-section for oblique seas

Table 5.6: Mean and standard deviation error for torsional bending moments

Mx	Mid	Mean error	Standard deviation error
S004	Cond2	-99%	2%
S004	Cond4	-102%	-4%
S004	Cond6	-102%	-4%
S006	Cond9	-95%	55%
S006	Cond11	-103%	39%
S008	Cond14	-101%	5%
S008	Cond16	-100%	35%

5.3.8 Discussion of results

The numerical seakeeping simulation has taken the experimental results as a reference in its analysis. Uncertainties due to the numerical simplifications in the discrete mass distribution and hull shape could be a reason for inconsistencies, since there will always be differences between the segmented and numerical models (Zhu et al. 2011a). As observed, the accuracy of the simulation set up of the draft could be a factor of discrepancy in the results. Some differences in the mean values of heave motion and shear forces could be partly to the result an uncertainty in the real position of draft, fixed for the experiment. A misrepresentation in the scaling of the real position of the cross-section could also add to the geometric uncertainty.

The rigidity of the model compromises the prediction of the numerical results, as it can be seen in the roll motion. The flexibility of the segmented model, characterized by its stiffness in the different segments, shows a more sensible reading of the data due to the response of each segment to the waves. Whereas the numerical model provides a more predictable pattern that ends, due to its rigidity, overestimating the real standard deviation of the experiment.

The use of linear wave theory by the simulations starts compromising the results on higher sea states and at higher speeds, where there is a rougher interaction between hull and wave. In these cases, nonlinearities are also introduced, producing higher differences with the simulation results. Other effects not considered in the simulations as roll damping are also factors on the accuracy of the numerical results.

The characteristics of the set up for the seakeeping analysis are described in previous chapters, as well as for the main characteristics for the Rankine panel grid and the properties of the motion springs used for the simulations. Considering the software, the interpretation of the JONSWAP definition by Wasim reproduces with discrepancies the induced waves of the short-crested sea states. This effect is later reflected in the motion and loads.

Even though in some conditions there are some deviations, between the models, the simulated results can be considered to be close to the one measured on the experiment working as a good predicament of the segmented model behavior. The simulated shear forces and vertical bending moments for all sea states are within 7% of mean error from the experimental values. At the same time, the prediction at short vessel speed is accurate showing that this at under slow velocities even in high seas such as in S008Cond13 and S008Cond14; there are good agreements.

The seakeeping numerical simulations work well for the motions and loads presented. The set-up choice used in the analysis show good agreements in the prediction of the motions and loads presented, especially in lower sea states and at low speed. Regarding the torsional moment, even if there is a clear need for more accuracy the response can work as an initial indicator. For a better analysis of higher sea states at higher vessel speeds, it would be recommended to introduce roll damping as well as small nonlinearities in the simulation.

6 Conclusions

This work has focused on the assessment of the simulations of a rigid numerical model against the experimental segmented model test. The goal has been to understand where limits are with the simulations, and under which conditions can the simulation reproduce the experimental behavior. The thesis work used insights from literature and the experiment to understand and prepare the numerical simulation and its following assessment analysis.

The eigenfrequency simulation result agrees well with the hammer test result in wet conditions. The rigid model with a discrete mass distribution along the hull has proven to be in good agreement with the experimental test; with a natural frequency of 0.79 Hz, having the model is an 8% of difference to the experimental value. The discrepancy between the model's frequencies could be due to several sources, such as the simplified mass distribution and the rigidity of the model. Other sources of divergence could also be due to uncertainties in the hammer test experiment. However, the simulated dry frequency differs significantly from the experimental eigenfrequency. An indicative frequency of 1.13 Hz, calculated through an approximation, has been presented.

For the seakeeping simulations, good agreements have been found with the different sea states on the analysis. This correlation was found for all shear forces and bending moments in all sea states. This is due to the ability of the numerical model to read vertical loads in comparison with the heave motion, where the effect of a vertical offset could have affected the predictions. These similarities in the prediction were particularly found on lower sea states at lower speeds where the difference between models was minimal, due to the linearity of the waves and also the effects caused by the segmented model.

More discrepancies in the results were found at higher waves, and with higher speeds. Some limitations were found concerning the accuracy due to the linearity of the waves to define short crested conditions, which showed higher deviations in the prediction of the loads. However, it cannot be concluded that nonlinearity is the only factor of divergence. Other factors, such as the rigidity of the model, uncertainties in the experiment and mass distributions could have also affected the results. More significant differences are found in the torsional moments for which the rigid body model behaves much differently in comparison with the segmented model. Thus, the numerical model is not recommended for a torsion analysis; it is mainly applicable for analysing the vertical responses.

In summary, a numerical rigid model simulation is able to present a segmented model test behavior and to give accurate vertical responses. Comparing the numerical values with the experiment data one concludes that the numerical model achieves to capture the load response, especially in terms of vertical forces and moments. The model at the same time is limited by the linearity of the simulations starting to compromise the predictions at conditions higher seas and speed. The use of the model as the one in this thesis is a path to ensure a more straightforward analysis in an elaborated experimental model, helping shipbuilding focus on hull optimization. This model focuses on lightweight construction in combination with other mathematical approach to ship design the industry will response to the sustainability requirements of society.

7 Future work

In the current work, several different simplifications were made related to the numerical simulation set up to overcome specific difficulties and to facilitate the method. The use of linear wave theory proved to capture the vertical forces and moments, but it becomes less accurate at higher sea states with higher vessel speed. A more sophisticated numerical model that accounts more nonlinearities as well as other effects such as roll damping could give more convincing results when a rigid model is utilized.

The use of the SESAM software package helped the workflow in terms of compatibility between the programs used for the thesis. On the other hand, in the eigenanalysis, more sophisticated software such as ABAQUS is expected to be useful to compare with the GeniE results, by providing the use of free vibration as well as a more detailed mass distribution.

A fatigue assessment of dynamic loads could also add to the understanding of the ship dynamics' structural behavior into the long-term vessel operation. It would be interesting to know how the rigid body model could capture the dynamic effects such as springing or whipping. This study could be especially helpful in the investigation of the impacts of sea conditions such as the presented in this thesis.

9 References

- Aichun, F.; Wei, B.; You, Y.; Zhi-Min, C.; Price W.G. (2016). A Rankine source method solution of a finite depth, wave-body interaction problem. *Journal of Fluids and Structures* 62 p. 14-32.
- Appa Rao, T.V.S.R.; Iyer, N.R.; Rajasankar, J.; Palani, G.S. (2000). Dynamic Response Analysis of Ship Hull Structures. *Marine Technology* 37(3) p. 117-128.
- Beck, R.F. (1994) Time-domain computations for floating bodies. *Applied Ocean Research* 16 p. 267-282.
- Bertram, V. (2012). Practical Ship Hydrodynamics. 2nd. Oxford: Elsevier Ltd.
- Brodtkorb, P.A.; Johannesson, P.; Lindgren, G.; Rychlik, I.; Rydén, J.; Sjö, E. (2000). WAFO - a Matlab toolbox for analysis of random waves and loads. *Proceedings of the 10th International Offshore and Polar Engineering Conference* in Seattle, WA, United States.
- Chen, Z.; Jiao, J.; Li, H. (2017). Time-domain numerical and segmented ship model experimental analyses of hydroelastic responses of a large container ship in oblique regular waves. *Applied Ocean Research* 67 p. 78-93.
- Davies, E.A.J.; Woodward, J.B.; Vance, J.E.; Stilwell, J.J. (2018). Encyclopædia Britannica. <https://www.britannica.com/technology/ship> (accessed May 22, 2019).
- Dinsbacher, A.; Engle, A.; Hermanski, G. (2010). Guidelines for Hydroelastic Model Design, Testing and Analysis of Loads and Responses. *Report No. NSWCCD-65-TR2010/12* (Report No. NSWCCD-65-TR2010/1), no. Carderock Div, NSW.
- DNV GL. (2015). Genie V7.2-07. *DNV GL - Software*.
- DNV GL. (2016). HydroD V.4.9-02. *DNV GL Software SESAM*.
- DNV GL. (2015). SESAM USER MANUAL. WASIM Wave Loads on Vessels with Forward Speed. *DNV GL - Software*.
- DNV. (2006). SESAM User Manual Wasim. 5th. Horvik: Det Norske Veritas.
- Fonseca, N.; Soares, C.G. (2004). Experimental Investigation of the Nonlinear Effects on the Statistics of Vertical Motions and Loads of a Containership in Irregular Waves. *Journal of Ship Research*. 48 (2) p. 148-167.
- Groenenboom, P.; Cartwright, B.; McGuckin, D. (2009). Numerical Simulation Of Ships In High Seas Using A Coupled SPH-FE Approach. *Fremantle: The Royal Institution of Naval Architects*.
- Hong, S.Y.; Kim, B.W.; Nam, B.W. (2011). Experimental study on torsion springing and whipping of a large container ship. *Proceedings of the International Offshore and Polar Engineering Conference (21st International Offshore and Polar Engineering Conference)* in Maui, HI; United States p. 486-494.
- IMO. (2017) IMO and Sustainable Development. <http://www.imo.org/en/MediaCentre/HotTopics/Documents/IMO%20SDG%20Brochure.pdf> (accessed April 1, 2019).

ITTC. (2011) ITTC – Recommended Procedures and Guidelines: Global Loads Seakeeping Procedure. 26th ITTC Seakeeping Committee.

Jiao, J.; Chen, C.; Ren, H. (2019) A comprehensive study on ship motion and load responses in short-crested irregular waves. *International Journal of Naval Architecture and Ocean Engineering* 11(1) p. 364 - 379.

Jung-Hyun, K.; Kim, Y.; Yuck, R-H.; Lee, D-Y. (2015). Comparison of slamming and whipping loads by fully coupled hydroelastic analysis and experimental measurement. *Journal of Fluids and Structures* 52 p. 145-165.

Li, Z.; Mao, W.; Ringsberg, J.W.; Johnson, E.; Storhaug, G. (2014). A comparative study of fatigue assessments of container ship structures using various direct calculation approaches. *Ocean Engineering* 82(15) p. 65-74.

Lin, W-M.; Weems, K.M.; Liut D.A. (2004). Design and Assessment of Ship Motion Control Systems with Advanced Numerical Simulation Tools. *Habitability of Combat and Transport Vehicles: Noise, Vibration and Motion (RTO-MP-AVT-110)*. in Prague, Czech Republic, 2004.

Marón, A.; Kapsenberg, G. (2014). Design of a ship model for hydro-elastic experiments in waves. *International Journal of Naval Architecture and Ocean Engineering* 5(4) p. 1130-1147.

Mathworks. (2016) Matlab R2016b. Mathworks, Inc.

Norwood, M.N.; Dow, R.S. (2013) Dynamic analysis of ship structures. *Ships and Offshore Structures* 8(3-4) p. 270-288.

Perez, T. (2015). Ship Motion Control: Course Keeping and Roll Stabilisation Using Rudders and Fins. *First. Trondheim: Springer*.

Sader, J.E. (1998). Frequency response of cantilever beams immersed in viscous fluids with applications to the atomic force microscope. *Journal of Applied Physics* 84(1) p. 64-76.

Singh, S.P.; Sen, D. (2007). A comparative linear and nonlinear ship motion study using 3-D time domain methods. *Ocean Engineering* 34(13) p. 1863-1881.

Stena Teknik. (2019). Take A Glimpse At Our Projects. <https://www.stenateknik.com/projects/> (accessed April 4, 2019).

Storhaug, G. (2014). The measured contribution of whipping and springing on the fatigue and extreme loading of container vessels. *International Journal of Naval Architecture and Ocean Engineering* 6(4) p. 1096-1110.

Temarel, P.; Bai, W.; Bruns, A.; Derbanne, Q.; Dessi, D.; Dhavalikar, S.; Fonseca, N.; Fukasawa, T.; Gu, X.; Nestegard, A.; Papanikolaou, A.; Song, K.H.; Wang, S. (2016). Prediction of wave-induced loads on ships: Progress and challenges. *Ocean Engineering* 116 p. 274-308.

United Nations. (2015). Resolution adopted by the General Assembly on 25 September 2015. October 21, 2015. http://www.un.org/ga/search/view_doc.asp?symbol=A/RES/70/1&Lang=E (accessed April 1, 2019).

United Nations.(2019). Sustainable Development Goals: 17 Goals to Transform Our World. <https://www.un.org/sustainabledevelopment/> (accessed April 2, 2019).

Vakilabadi, K.A.; Khedmati, M.A.; Sayyari, A. (2014). Analysis of the flexural mode response of a novel trimaran by segmented model test." *Latin American Journal of Solids and Structures* 14(11) p. 2573-2588.

Veryst Engineering. (2019). Immersed Beam Vibration. <https://www.veryst.com/project/immersed-beam-vibration> (accessed March 2019-03-20, 2019).

Zhu, S.; Wu, MK.; Moan, T. (2011). Experimental and Numerical Study of Wave-Induced Load Effects of Open Ships in Oblique Seas. *Journal of Ship Research* 55(2) p. 100-123.

Zhu, S.; Wu, MK.; Moan, T. (2011) Experimental Investigation of Hull Girder Vibrations of a Flexible Backbone Model in Bending and Torsion. *Applied Ocean Research*, p. 252-272.

A. Statistical data of the numerical and experimental results

In this appendix lists, tables regarding the results for each seakeeping running condition from the experiment and simulations are presented. Showing the maximum, minimum, mean and standard deviation for all sea state conditions. At the same time the numerical difference in results with the experiments is also presented. The seakeeping wave basin test runs used for comparison in the thesis are also showcased. The order followed is the same as the one presented in Table 4.3.

A.1 S004

A.1.1 Condition 1

The experimental tests compared against are:

- Ser004-Test001-Run001
- Ser004-Test001-Run002
- Ser004-Test002-Run001

Table A.1 Properties for S004Cond1

Sea state	S004
Speed (Kts)	15
Wave direction (deg)	180
Significant wave height (m)	1,88
Wave period (s)	7,56

Table A.2: Statistical data of the experiment for S004Cond1

S004Cond1	Min	Mean	Max	Standard deviation
Wave elevation (m)	-1,62	0,00	1,32	0,43
Surge (m)	-0,08	0,08	0,48	0,10
Sway (m)	-0,17	0,01	0,25	0,07
Heave (m)	-0,01	0,14	0,26	0,04
Roll (deg)	-0,45	0,06	0,53	0,19
Pitch (deg)	-0,17	0,04	0,21	0,06
Yaw (deg)	0,00	0,00	0,26	0,08
Mid cut Fx (N)	7,98E+06	8,30E+06	8,64E+06	1,08E+05
Mid cut Fy (N)	-2,75E+06	-2,44E+06	-2,12E+06	1,03E+05
Mid cut Fz (N)	-1,31E+07	-1,13E+07	-9,30E+06	6,39E+05
Mid cut Mx (Nm)	-3,31E+06	-4,43E+04	2,93E+06	9,21E+05
Mid cut My (Nm)	-9,31E+08	-8,31E+08	-7,34E+08	3,21E+07
Mid cut Mz (Nm)	-3,31E+06	-4,43E+04	2,93E+06	9,21E+05

Table A.3: Statistical data of the simulation for S004Cond1

S004Cond1	Min	Mean	Max	Standard deviation	Mean difference	Std. deviation difference
Wave elevation (m)	-1,34	0,00	1,13	0,42	-0,14	-0,03
Surge (m)	-0,06	0,11	0,48	0,11	0,40	0,07
Sway (m)	-0,15	0,01	0,12	0,05	0,30	-0,21
Heave (m)	0,02	0,14	0,25	0,04	0,03	0,00
Roll (deg)	-0,45	0,06	0,53	0,19	0,01	0,03
Pitch (deg)	-0,15	0,04	0,21	0,06	-0,01	0,00
Yaw (deg)	0,00	0,00	0,20	0,07	0,86	-0,12
Mid cut Fx (N)	7,98E+06	8,30E+06	8,63E+06	1,10E+05	3,41E-04	1,71E-02
Mid cut Fy (N)	-2,75E+06	-2,44E+06	-2,12E+06	1,07E+05	-1,19E-04	4,03E-02
Mid cut Fz (N)	-1,31E+07	-1,13E+07	-9,30E+06	6,41E+05	-1,52E-04	3,09E-03
Mid cut Mx (Nm)	-3,31E+06	-4,70E+04	2,93E+06	9,61E+05	5,97E-02	4,28E-02
Mid cut My (Nm)	-9,31E+08	-8,31E+08	-7,34E+08	3,27E+07	-3,76E-04	1,89E-02
Mid cut Mz (Nm)	-3,31E+06	-4,70E+04	2,93E+06	9,61E+05	5,97E-02	4,28E-02

A.1.2 Condition 2

The experimental tests compared against are:

- Ser004-Test003-Run001
- Ser004-Test004-Run002
- Ser004-Test005-Run001

Table A.4: Properties for S004Cond2

Sea state	S004
Speed (Kts)	15
Wave direction (deg)	150
Significant wave height (m)	1,88
Wave period (s)	7,56

Table A.5: Statistical data of the experiment for S004Cond2

S004Cond2	Min	Mean	Max	Standard deviation
Wave elevation (m)	-1,62	0,02	1,56	0,46
Surge (m)	-0,39	0,01	0,31	0,17
Sway (m)	-0,37	0,05	0,48	0,26
Heave (m)	-0,07	0,16	0,37	0,07
Roll (deg)	-1,06	-0,21	0,75	0,27
Pitch (deg)	-0,31	0,04	0,36	0,11
Yaw (deg)	-0,01	-0,01	0,45	0,25
Mid cut Fx (N)	7,76E+06	8,29E+06	8,90E+06	1,53E+05
Mid cut Fy (N)	-4,08E+06	-2,41E+06	-9,96E+05	3,93E+05
Mid cut Fz (N)	-1,37E+07	-1,13E+07	-8,17E+06	7,68E+05
Mid cut Mx (Nm)	-1,33E+07	-7,33E+05	1,11E+07	3,08E+06
Mid cut My (Nm)	-9,93E+08	-8,31E+08	-6,18E+08	4,85E+07
Mid cut Mz (Nm)	-1,33E+07	-7,33E+05	1,11E+07	3,08E+06

Table A.6: Statistical data of the simulation for S004Cond2

S004Cond2	Min	Mean	Max	Standard deviation	Mean difference	Std. deviation difference
Wave elevation (m)	-1,52	0,00	1,55	0,47	-0,98	0,04
Surge (m)	-0,40	-0,28	-0,17	0,05	-29,43	-0,71
Sway (m)	-0,27	-0,03	0,17	0,11	-1,54	-0,58
Heave (m)	-0,13	0,12	0,37	0,09	-0,25	0,29
Roll (deg)	-1,25	0,00	1,00	0,31	-1,01	0,14
Pitch (deg)	-0,46	0,00	0,39	0,15	-0,96	0,40
Yaw (deg)	0,00	0,00	0,05	0,02	-1,35	-0,91
Mid cut Fx (N)	3,72E+06	4,27E+06	4,84E+06	1,81E+05	-4,85E-01	1,82E-01
Mid cut Fy (N)	-1,15E+06	-6,92E+02	1,03E+06	3,31E+05	-1,00E+00	-1,56E-01
Mid cut Fz (N)	-1,30E+07	-1,06E+07	-8,15E+06	6,05E+05	-6,27E-02	-2,11E-01
Mid cut Mx (Nm)	-1,28E+07	-8,19E+03	1,47E+07	3,14E+06	-9,89E-01	2,21E-02
Mid cut My (Nm)	-9,01E+08	-7,90E+08	-4,87E+10	3,98E+07	-5,05E-02	-1,79E-01
Mid cut Mz (Nm)	-4,20E+07	-7,24E+04	3,79E+07	1,37E+07	-9,01E-01	3,44E+00

A.1.3 Condition 3

The experimental tests compared against are:

- Ser004-Test006-Run001
- Ser004-Test008-Run002
- Ser004-Test010-Run001

Table A.7: Properties for S004Cond3

Sea state	S004
Speed (Kts)	18
Wave direction (deg)	180
Significant wave height (m)	1,88
Wave period (s)	7,56

Table A.8: Statistical data of the experiment for S004Cond3

S004Cond1	Min	Mean	Max	Standard deviation
Wave elevation (m)	-1,63	0,01	1,64	0,48
Surge (m)	-0,26	0,00	0,21	0,09
Sway (m)	-0,16	0,00	0,18	0,06
Heave (m)	0,01	0,20	0,34	0,05
Roll (deg)	-0,38	0,04	0,47	0,14
Pitch (deg)	-0,18	0,04	0,27	0,07
Yaw (deg)	0,00	0,00	0,23	0,10
Mid cut Fx (N)	8,08E+06	8,47E+06	8,84E+06	1,24E+05
Mid cut Fy (N)	-2,79E+06	-2,43E+06	-2,06E+06	1,01E+05
Mid cut Fz (N)	-1,32E+07	-1,11E+07	-8,54E+06	7,19E+05
Mid cut Mx (Nm)	-3,40E+06	7,30E+03	3,13E+06	8,63E+05
Mid cut My (Nm)	-9,19E+08	-8,17E+08	-6,86E+08	3,75E+07
Mid cut Mz (Nm)	-3,40E+06	7,30E+03	3,13E+06	8,63E+05

Table A.9: Statistical data of the simulation for S004Cond3

S004Cond3	Min	Mean	Max	Standard deviation	Mean difference	Std. deviation difference
Wave elevation (m)	-1,73	0,00	1,53	0,47	-1,02	-0,02
Surge (m)	0,03	0,16	0,31	0,06	-45,48	-0,38
Sway (m)	0,00	0,00	0,00	0,00	-1,00	-1,00
Heave (m)	-0,06	0,12	0,32	0,06	-0,38	0,34
Roll (deg)	0,00	0,00	0,00	0,00	-1,00	-1,00
Pitch (deg)	-0,30	0,00	0,27	0,10	-0,94	0,48
Yaw (deg)	0,00	0,00	0,00	0,00	-1,00	-1,00
Mid cut Fx (N)	3,78E+06	4,27E+06	4,71E+06	1,46E+05	-4,96E-01	1,75E-01
Mid cut Fy (N)	-1,72E+01	1,13E-02	2,07E+01	4,02E+00	-1,00E+00	-1,00E+00
Mid cut Fz (N)	-1,34E+07	-1,06E+07	-7,97E+06	6,55E+05	-4,51E-02	-8,89E-02
Mid cut Mx (Nm)	3,09E+03	3,75E+03	4,43E+03	2,09E+02	-4,86E-01	-1,00E+00
Mid cut My (Nm)	-9,01E+08	-7,89E+08	-6,68E+08	3,40E+07	-3,37E-02	-9,31E-02
Mid cut Mz (Nm)	-7,51E+02	1,33E+01	7,88E+02	2,20E+02	-9,98E-01	-1,00E+00

A.1.4 Condition 4

The experimental tests compared against are:

- Ser004-Test015-Run001
- Ser004-Test016-Run002
- Ser004-Test017-Run001

Table A.10: Properties for S004Cond4

Sea state	S004
Speed (Kts)	18
Wave direction (deg)	150
Significant wave height (m)	1,88
Wave period (s)	7,56

Table A.11: Statistical data of the experiment for S004Cond4

S004Cond1	Min	Mean	Max	Standard deviation
Wave elevation (m)	-2,19	0,00	1,46	0,48
Surge (m)	-0,22	-0,01	0,20	0,09
Sway (m)	-0,33	0,06	0,43	0,14
Heave (m)	0,05	0,22	0,42	0,06
Roll (deg)	-0,38	0,20	1,02	0,22
Pitch (deg)	-0,32	0,04	0,42	0,11
Yaw (deg)	-0,02	-0,02	0,53	0,20
Mid cut Fx (N)	8,01E+06	8,45E+06	8,99E+06	1,69E+05
Mid cut Fy (N)	-3,58E+06	-2,39E+06	-1,13E+06	3,79E+05
Mid cut Fz (N)	-1,32E+07	-1,11E+07	-8,65E+06	7,40E+05
Mid cut Mx (Nm)	-1,27E+07	-7,15E+05	1,07E+07	3,18E+06
Mid cut My (Nm)	-9,59E+08	-8,17E+08	-6,81E+08	5,05E+07
Mid cut Mz (Nm)	-1,27E+07	-7,15E+05	1,07E+07	3,18E+06

Table A.12: Statistical data of the simulation for S004Cond4

S004Cond4	Min	Mean	Max	Standard deviation	Mean difference	Std. deviation difference
Wave elevation (m)	-1,62	0,00	1,48	0,47	-1,57	-0,01
Surge (m)	0,20	0,28	0,35	0,03	-31,83	-0,67
Sway (m)	-0,11	0,00	0,09	0,03	-1,06	-0,78
Heave (m)	-0,13	0,12	0,38	0,09	-0,43	0,37
Roll (deg)	-0,76	0,00	0,75	0,25	-1,00	0,10
Pitch (deg)	-0,42	0,00	0,34	0,14	-0,96	0,35
Yaw (deg)	0,00	0,00	0,02	0,00	-1,04	-0,98
Mid cut Fx (N)	3,57E+06	4,27E+06	4,83E+06	1,86E+05	-4,95E-01	1,06E-01
Mid cut Fy (N)	-1,00E+06	1,51E+03	9,10E+05	3,31E+05	-1,00E+00	-1,27E-01
Mid cut Fz (N)	-1,29E+07	-1,06E+07	-8,40E+06	6,18E+05	-4,54E-02	-1,65E-01
Mid cut Mx (Nm)	-9,66E+06	1,61E+04	1,18E+07	3,06E+06	-1,02E+00	-3,93E-02
Mid cut My (Nm)	-9,17E+08	-7,89E+08	-6,51E+08	4,03E+07	-3,36E-02	-2,01E-01
Mid cut Mz (Nm)	-4,30E+07	2,25E+04	4,57E+07	1,40E+07	-1,03E+00	3,39E+00

A.1.5 Condition 5

The experimental tests compared against are:

- Ser004-Test015-Run024
- Ser004-Test016-Run025

Table A.13: Properties for S004Cond5

Sea state	S004
Speed (Kts)	21
Wave direction (deg)	180
Significant wave height (m)	1,88
Wave period (s)	7,56

Table A.14: Statistical data of the experiment for S004Cond5

S004Cond5	Min	Mean	Max	Standard deviation
Wave elevation (m)	-1,42	0,02	1,10	0,47
Surge (m)	-0,19	-0,07	0,02	0,06
Sway (m)	-0,18	0,01	0,15	0,09
Heave (m)	0,16	0,27	0,36	0,04
Roll (deg)	-0,26	0,01	0,22	0,10
Pitch (deg)	-0,11	0,05	0,20	0,06
Fore cut Mz (Nm)	-9,10E+04	-6,19E+04	-2,91E+04	9,49E+03
Mid cut Fx (N)	8,37E+06	8,69E+06	9,03E+06	1,28E+05
Mid cut Fy (N)	-2,65E+06	-2,40E+06	-2,20E+06	8,25E+04
Mid cut Fz (N)	-1,27E+07	-1,07E+07	-8,71E+06	7,97E+05
Mid cut Mx (Nm)	-2,34E+06	1,77E+04	1,75E+06	7,17E+05
Mid cut My (Nm)	-9,23E+08	-8,01E+08	-6,89E+08	4,05E+07

Table A.15: Statistical data of the simulation for S004Cond5

S004Cond5	Min	Mean	Max	Standard deviation	Mean difference	Std. deviation difference
Wave elevation (m)	-1,41	0,00	1,64	0,43	-0,95	-0,07
Surge (m)	-0,13	-0,10	-0,06	0,02	0,38	-0,74
Sway (m)	0,00	0,00	0,00	0,00	-1,00	-1,00
Heave (m)	-0,01	0,12	0,26	0,06	-0,53	0,32
Roll (deg)	0,00	0,00	0,00	0,00	-1,00	-1,00
Pitch (deg)	-0,19	0,00	0,19	0,09	-0,97	0,47
Fore cut Mz (Nm)	-1,21E+00	-7,83E-03	1,08E+00	3,68E-01	-1,00E+00	-1,00E+00
Mid cut Fx (N)	3,81E+06	4,27E+06	4,68E+06	1,47E+05	-5,09E-01	1,49E-01
Mid cut Fy (N)	-1,23E+01	4,64E-03	1,33E+01	4,10E+00	-1,00E+00	-1,00E+00
Mid cut Fz (N)	-1,32E+07	-1,06E+07	-8,02E+06	6,78E+05	-1,69E-02	-1,49E-01
Mid cut Mx (Nm)	-4,30E+03	3,75E+03	-3,09E+03	2,01E+02	-7,88E-01	-1,00E+00
Mid cut My (Nm)	-8,92E+08	-7,89E+08	-6,79E+08	3,61E+07	-1,43E-02	-1,08E-01

A.1.6 Condition 6

The experimental tests compared against are:

- Ser004-Test026-Run001
- Ser004-Test027-Run001
- Ser004-Test028-Run001

Table A.16: Properties for S004Cond6

Sea state	S004
Speed (Kts)	21
Wave direction (deg)	150
Significant wave height (m)	1,88
Wave period (s)	7,56

Table A.17: Statistical data of the experiment for S004Cond6

S004Cond6	Min	Mean	Max	Standard deviation
Wave elevation (m)	-2,19	0,00	1,46	0,48
Surge (m)	-0,22	-0,01	0,20	0,09
Sway (m)	-0,33	0,06	0,43	0,14
Heave (m)	0,05	0,22	0,42	0,06
Roll (deg)	-0,38	0,20	1,02	0,22
Pitch (deg)	-0,32	0,04	0,42	0,11
Fore cut Mz (Nm)	-2,20E+05	-8,32E+04	3,14E+04	3,01E+04
Mid cut Fx (N)	8,01E+06	8,45E+06	8,99E+06	1,69E+05
Mid cut Fy (N)	-3,58E+06	-2,39E+06	-1,13E+06	3,79E+05
Mid cut Fz (N)	-1,32E+07	-1,11E+07	-8,65E+06	7,40E+05
Mid cut Mx (Nm)	-1,27E+07	-7,15E+05	1,07E+07	3,18E+06
Mid cut My (Nm)	-9,59E+08	-8,17E+08	-6,81E+08	5,05E+07

Table A.18: Statistical data of the simulation for S004Cond6

S004Cond6	Min	Mean	Max	Standard deviation	Mean difference	Std. deviation difference
Wave elevation (m)	-1,62	0,00	1,48	0,47	-1,57	-0,01
Surge (m)	0,20	0,28	0,35	0,03	-31,83	-0,67
Sway (m)	-0,11	0,00	0,09	0,03	-1,06	-0,78
Heave (m)	-0,13	0,12	0,38	0,09	-0,43	0,37
Roll (deg)	-0,76	0,00	0,75	0,25	-1,00	0,10
Pitch (deg)	-0,42	0,00	0,34	0,14	-0,96	0,35
Fore cut Mz (Nm)	-3,53E+01	6,59E-02	4,27E+01	1,23E+01	-1,00E+00	-1,00E+00
Mid cut Fx (N)	3,57E+06	4,27E+06	4,83E+06	1,86E+05	-4,95E-01	1,06E-01
Mid cut Fy (N)	-1,00E+06	1,51E+03	9,10E+05	3,31E+05	-1,00E+00	-1,27E-01
Mid cut Fz (N)	-1,29E+07	-1,06E+07	-8,40E+06	6,18E+05	-4,54E-02	-1,65E-01
Mid cut Mx (Nm)	-9,66E+06	1,61E+04	1,18E+07	3,06E+06	-1,02E+00	-3,93E-02
Mid cut My (Nm)	-9,17E+08	-7,89E+08	-6,51E+08	4,03E+07	-3,36E-02	-2,01E-01

A.2 S005

A.2.1 Condition 7

The experimental tests compared against are:

- Ser005-Test001-Run001
- Ser005-Test002-Run001
- Ser005-Test007-Run001

Table A.19: Properties for S005Cond7

Sea state	S005
Speed (Kts)	18
Wave direction (deg)	180
Significant wave height (m)	1,88
Wave period (s)	4

Table A.20: Statistical data of the experiment for S005Cond7

S005Cond7	Min	Mean	Max	Standard deviation
Wave elevation (m)	-1,9099	0,063881	1,410456	0,37
Surge (m)	-0,24959	-0,00838	0,102388	0,05
Sway (m)	-0,13875	0,000631	0,190165	0,06
Heave (m)	0,209872	0,243279	0,26789	0,01
Roll (deg)	-0,115	0,040087	0,24	0,08
Pitch (deg)	0	0,03612	0,065	0,01
Yaw (deg)	0,003494	0,003494	0,22	0,13
Mid cut Fx (N)	8,31E+06	8,50E+06	8,66E+06	5,07E+04
Mid cut Fy (N)	-2,58E+06	-2,44E+06	-2,33E+06	3,95E+04
Mid cut Fz (N)	-1,14E+07	-1,11E+07	-1,08E+07	1,03E+05
Mid cut Mx (Nm)	-1,65E+06	-1,39E+05	1,25E+06	4,21E+05
Mid cut My (Nm)	-8,56E+08	-8,18E+08	-7,76E+08	1,15E+07
Mid cut Mz (Nm)	-1,65E+06	-1,39E+05	1,25E+06	4,21E+05

Table A.21: Statistical data of the simulation for S005Cond7

S005Cond7	Min	Mean	Max	Standard deviation	Mean difference	Std. deviation difference
Wave elevation (m)	-1,48	0,00	1,65	0,46	-0,99	0,27
Surge (m)	1,10	3,11	5,33	1,26	-372,45	23,07
Sway (m)	-0,11	0,03	0,16	0,06	39,52	0,08
Heave (m)	0,21	0,22	0,24	0,01	-0,08	-0,27
Roll (deg)	-0,21	0,01	0,31	0,09	-0,76	0,17
Pitch (deg)	-0,04	0,00	0,03	0,01	-1,09	0,04
Yaw (deg)	-0,01	-0,01	0,02	0,01	-4,18	-0,91
Mid cut Fx (N)	4,06E+06	4,26E+06	4,47E+06	6,34E+04	-0,50	0,25
Mid cut Fy (N)	-4,00E+05	-2,72E+03	5,73E+05	1,54E+05	-1,00	2,88
Mid cut Fz (N)	-1,12E+07	-1,05E+07	-9,79E+06	1,94E+05	-0,05	0,88
Mid cut Mx (Nm)	-5,20E+06	-3,39E+04	5,69E+06	1,43E+06	-0,76	2,39
Mid cut My (Nm)	-8,25E+08	-7,89E+08	-7,49E+08	1,06E+07	-0,04	-0,08
Mid cut Mz (Nm)	-2,41E+07	-5,45E+04	2,58E+07	7,98E+06	-0,61	17,96

A.3 S006

A.3.1 Condition 8

The experimental tests compared against are:

- Ser006-Test002-Run001
- Ser006-Test009-Run001
- Ser006-Test010-Run001

Table A.22: Properties for S006Cond8

Sea state	S006
Speed (Kts)	18
Wave direction (deg)	150
Significant wave height (m)	3,25
Wave period (s)	9,24

Table A.23: Statistical data of the experiment for S006Cond8

S006Cond8	Min	Mean	Max	Standard deviation
Wave elevation (m)	-3,24359	0,072949	2,277077	0,77
Surge (m)	-0,749	-0,0009	0,370811	0,22
Sway (m)	-0,44142	-0,01185	0,390555	0,13
Heave (m)	-0,26842	0,250548	0,703848	0,17
Roll (deg)	-0,87	0,03425	0,945	0,30
Pitch (deg)	-0,83	0,052067	0,985	0,30
Yaw (deg)	0,013258	0,013258	0,52	0,16
Mid cut Fx (N)	7,53E+06	8,61E+06	1,03E+07	4,20E+05
Mid cut Fy (N)	-3,09E+06	-2,43E+06	-1,63E+06	2,35E+05
Mid cut Fz (N)	-1,50E+07	-1,11E+07	-6,79E+06	1,53E+06
Mid cut Mx (Nm)	-4,56E+06	-8,21E+04	4,83E+06	1,57E+06
Mid cut My (Nm)	-1,18E+09	-8,12E+08	-4,41E+08	1,21E+08
Mid cut Mz (Nm)	-4,56E+06	-8,21E+04	4,83E+06	1,57E+06

Table A.24: Statistical data of the simulation for S006Cond8

S006Cond8	Min	Mean	Max	Standard deviation	Mean difference	Std. deviation difference
Wave elevation (m)	-2,84	0,00	3,02	0,82	-0,97	0,06
Surge (m)	-0,04	0,28	0,63	0,12	-311,12	-0,45
Sway (m)	0,00	0,00	0,00	0,00	-1,00	-1,00
Heave (m)	-0,67	0,12	0,96	0,29	-0,51	0,69
Roll (deg)	0,00	0,00	0,00	0,00	-1,00	-1,00
Pitch (deg)	-1,41	0,00	1,36	0,49	-0,94	0,63
Yaw (deg)	0,00	0,00	0,00	0,00	-1,00	-1,00
Mid cut Fx (N)	2,88E+06	4,27E+06	5,71E+06	4,86E+05	-0,50	0,16
Mid cut Fy (N)	-2,85E+01	-2,88E-02	3,54E+01	8,59E+00	-1,00	-1,00
Mid cut Fz (N)	-1,58E+07	-1,06E+07	-6,39E+06	1,30E+06	-0,05	-0,15
Mid cut Mx (Nm)	-1,29E+03	-3,75E+03	6,31E+03	8,18E+02	-0,95	-1,00
Mid cut My (Nm)	-1,12E+09	-7,90E+08	-5,00E+08	9,96E+07	-0,03	-0,17
Mid cut Mz (Nm)	-1,90E+03	-1,15E+00	2,39E+03	6,10E+02	-1,00	-1,00

A.3.2 Condition 9

The experimental tests compared against are:

- Ser006-Test016-Run001
- Ser006-Test020-Run001
- Ser006-Test020-Run001

Table A.25: Properties for S006Cond9

Sea state	S006
Speed (Kts)	18
Wave direction (deg)	150
Significant wave height (m)	3,25
Wave period (s)	9,24

Table A.26: Statistical data of the experiment for S006Cond9

S006Cond9	Min	Mean	Max	Standard deviation
Wave elevation (m)	-2,49997	0,056267	1,936718	0,73
Surge (m)	-0,72395	0,165184	0,884315	0,36
Sway (m)	-0,92923	0,025314	1,367124	0,50
Heave (m)	-0,32311	0,245451	0,779939	0,20
Roll (deg)	-1,395	0,27333	1,585	0,49
Pitch (deg)	-1,015	0,059751	1,19	0,39
Yaw (deg)	-0,02539	-0,02539	1,25	0,48
Mid cut Fx (N)	7,60E+06	8,64E+06	9,97E+06	4,20E+05
Mid cut Fy (N)	-3,87E+06	-2,37E+06	-3,37E+05	6,32E+05
Mid cut Fz (N)	-1,42E+07	-1,11E+07	-7,64E+06	1,16E+06
Mid cut Mx (Nm)	-1,72E+07	-1,00E+06	1,37E+07	5,21E+06
Mid cut My (Nm)	-1,13E+09	-8,11E+08	-4,88E+08	1,16E+08
Mid cut Mz (Nm)	-1,72E+07	-1,00E+06	1,37E+07	5,21E+06

Table A.27: Statistical data of the simulation for S006Cond9

S006Cond9	Min	Mean	Max	Standard deviation	Mean difference	Std. deviation difference
Wave elevation (m)	-3,17	0,00	2,29	0,81	-0,97	0,11
Surge (m)	-0,15	0,26	0,77	0,17	0,60	-0,52
Sway (m)	-2,46	-0,05	1,79	1,06	-2,81	1,10
Heave (m)	-0,78	0,12	0,97	0,34	-0,50	0,72
Roll (deg)	-3,32	0,01	3,19	1,21	-0,96	1,47
Pitch (deg)	-1,39	0,00	1,38	0,56	-0,93	0,43
Yaw (deg)	0,01	0,01	0,56	0,23	-1,24	-0,52
Mid cut Fx (N)	2,55E+06	4,27E+06	5,73E+06	5,30E+05	-0,51	0,26
Mid cut Fy (N)	-1,91E+06	-2,52E+03	1,91E+06	6,77E+05	-1,00	0,07
Mid cut Fz (N)	-1,51E+07	-1,06E+07	-5,50E+06	1,09E+06	-0,04	-0,07
Mid cut Mx (Nm)	-2,51E+07	-4,66E+04	2,25E+07	8,09E+06	-0,95	0,55
Mid cut My (Nm)	-1,14E+09	-7,89E+08	-4,96E+08	1,00E+08	-0,03	-0,14
Mid cut Mz (Nm)	-8,64E+07	-3,87E+04	7,76E+07	3,01E+07	-0,96	4,79

A.3.3 Condition 10

The experimental tests compared against are:

- Ser006-Test006-Run001
- Ser006-Test007-Run001
- Ser006-Test020-Run001

Table A.28: Properties for S006Cond10

Sea state	S006
Speed (Kts)	15
Wave direction (deg)	180
Significant wave height (m)	3,25
Wave period (s)	9,24

Table A.29: Statistical data of the experiment for S006Cond10

S006Cond10	Min	Mean	Max	Standard deviation
Wave elevation (m)	-3,73193	0,057716	2,115221	0,75
Surge (m)	-0,47209	0,10784	0,497125	0,16
Sway (m)	-0,34889	-0,00823	0,357029	0,12
Heave (m)	-0,25853	0,201113	0,632527	0,16
Roll (deg)	-1,275	0,065571	1,445	0,46
Pitch (deg)	-0,73	0,049966	0,79	0,28
Yaw (deg)	0,003194	0,003194	0,265	0,12
Mid cut Fx (N)	7,49E+06	8,43E+06	9,61E+06	3,60E+05
Mid cut Fy (N)	-3,06E+06	-2,44E+06	-1,64E+06	2,52E+05
Mid cut Fz (N)	-1,48E+07	-1,12E+07	-7,06E+06	1,41E+06
Mid cut Mx (Nm)	-7,02E+06	-1,41E+05	7,86E+06	2,06E+06
Mid cut My (Nm)	-1,14E+09	-8,26E+08	-5,08E+08	1,09E+08
Mid cut Mz (Nm)	-7,02E+06	-1,41E+05	7,86E+06	2,06E+06

Table A.30: Statistical data of the simulation for S006Cond10

S006Cond10	Min	Mean	Max	Standard deviation	Mean difference	Std. deviation difference
Wave elevation (m)	-2,58	0,00	2,69	0,83	-0,97	0,10
Surge (m)	-0,04	0,28	0,65	0,13	1,58	-0,21
Sway (m)	0,00	0,00	0,00	0,00	-1,00	-1,00
Heave (m)	-0,57	0,12	0,82	0,26	-0,39	0,67
Roll (deg)	0,00	0,00	0,00	0,00	-1,00	-1,00
Pitch (deg)	-1,22	0,00	1,27	0,48	-0,96	0,70
Yaw (deg)	0,00	0,00	0,00	0,00	-1,00	-1,00
Mid cut Fx (N)	2,93E+06	4,27E+06	5,48E+06	4,56E+05	-0,49	0,27
Mid cut Fy (N)	-2,41E+01	3,86E-02	3,29E+01	9,08E+00	-1,00	-1,00
Mid cut Fz (N)	-1,53E+07	-1,06E+07	-5,77E+06	1,29E+06	-0,06	-0,09
Mid cut Mx (Nm)	-1,86E+03	-3,75E+03	5,74E+03	7,51E+02	-0,97	-1,00
Mid cut My (Nm)	-5,02E+08	-7,90E+08	-1,11E+09	1,02E+08	-0,04	-0,07
Mid cut Mz (Nm)	-1,91E+03	9,26E+00	2,06E+03	6,56E+02	-1,00	-1,00

A.3.4 Condition 11

The experimental tests compared against are:

- Ser006-Test003-Run002
- Ser005-Test004-Run002
- Ser005-Test005-Run001

Table A.31: Properties for S006Cond11

Sea state	S006
Speed (Kts)	15
Wave direction (deg)	150
Significant wave height (m)	3,25
Wave period (s)	9,24

Table A.32: Statistical data of the experiment for S006Cond11

S006Cond11	Min	Mean	Max	Standard deviation
Wave elevation (m)	-2,4787	0,039449	2,274302	0,79
Surge (m)	-1,09664	0,029133	0,725007	0,43
Sway (m)	-0,79264	0,073059	1,223466	0,46
Heave (m)	-0,4786	0,180948	0,822205	0,21
Roll (deg)	-1,39	0,289697	1,725	0,56
Pitch (deg)	-1,28	0,061485	1,42	0,45
Yaw (deg)	0,002305	0,002305	0,98	0,44
Mid cut Fx (N)	7,38E+06	8,43E+06	1,02E+07	4,50E+05
Mid cut Fy (N)	-4,63E+06	-2,41E+06	7,07E+03	7,33E+05
Mid cut Fz (N)	-1,50E+07	-1,13E+07	-7,12E+06	1,29E+06
Mid cut Mx (Nm)	-1,84E+07	-1,02E+06	1,59E+07	5,80E+06
Mid cut My (Nm)	-1,19E+09	-8,27E+08	-4,21E+08	1,36E+08
Mid cut Mz (Nm)	-1,84E+07	-1,02E+06	1,59E+07	5,80E+06

Table A.33: Statistical data of the simulation for S006Cond11

S006Cond11	Min	Mean	Max	Standard deviation	Mean difference	Std. deviation difference
Wave elevation (m)	-2,59	0,00	2,33	0,82	-0,95	0,04
Surge (m)	-0,05	0,27	0,65	0,13	8,40	-0,69
Sway (m)	-2,78	-0,20	1,63	1,06	-3,77	1,32
Heave (m)	-0,85	0,12	0,92	0,31	-0,32	0,49
Roll (deg)	-3,67	-0,02	3,30	1,36	-1,06	1,45
Pitch (deg)	-1,53	0,00	1,44	0,55	-0,99	0,23
Yaw (deg)	0,00	0,00	0,42	0,25	-1,25	-0,42
Mid cut Fx (N)	2,50E+06	4,27E+06	5,71E+06	5,04E+05	-0,49	0,12
Mid cut Fy (N)	-1,78E+06	-1,83E+02	1,78E+06	6,52E+05	-1,00	-0,11
Mid cut Fz (N)	-1,43E+07	-1,06E+07	-6,42E+06	1,08E+06	-0,06	-0,16
Mid cut Mx (Nm)	-2,40E+07	3,48E+04	2,22E+07	8,07E+06	-1,03	0,39
Mid cut My (Nm)	-1,15E+09	-7,89E+08	-4,85E+08	1,02E+08	-0,05	-0,25
Mid cut Mz (Nm)	-7,60E+07	1,75E+05	7,88E+07	2,80E+07	-1,17	3,83

A.4 S007

A.4.1 Condition 12

The experimental tests compared against are:

- Ser007-Test002-Run001
- Ser007-Test003-Run001
- Ser007-Test004-Run001

Table A.34: Properties for S007Cond12

Sea state	S007
Speed (Kts)	18
Wave direction (deg)	180
Significant wave height (m)	3,25
Wave period (s)	5

Table A.35: Statistical data of the experiment for S007Cond12

S007Cond12	Min	Mean	Max	Standard deviation
Wave elevation (m)	-2,29742	0,080143	2,513848	0,61
Surge (m)	-0,4014	-0,02541	0,237543	0,14
Sway (m)	-0,32136	-0,04231	0,280658	0,14
Heave (m)	0,164576	0,255713	0,332554	0,03
Roll (deg)	-0,475	0,075896	0,55	0,22
Pitch (deg)	-0,05	0,039297	0,125	0,03
Yaw (deg)	0,031508	0,031508	0,325	0,14
Mid cut Fx (N)	8,19E+06	8,52E+06	8,86E+06	8,88E+04
Mid cut Fy (N)	-2,89E+06	-2,42E+06	-2,06E+06	1,32E+05
Mid cut Fz (N)	-1,25E+07	-1,11E+07	-9,73E+06	3,54E+05
Mid cut Mx (Nm)	-3,91E+06	-1,74E+05	3,85E+06	1,40E+06
Mid cut My (Nm)	-8,87E+08	-8,16E+08	-7,46E+08	2,26E+07
Mid cut Mz (Nm)	-3,91E+06	-1,74E+05	3,85E+06	1,40E+06

Table A.36: Statistical data of the simulation for S007Cond12

S007Cond12	Min	Mean	Max	Standard deviation	Mean difference	Std. deviation difference
Wave elevation (m)	-2,54	0,00	3,03	0,74	-1,00	0,21
Surge (m)	0,42	1,15	1,59	0,36	-46,35	1,48
Sway (m)	-0,58	0,11	0,59	0,25	-3,58	0,78
Heave (m)	0,12	0,23	0,35	0,03	-0,11	0,32
Roll (deg)	-1,25	-0,02	1,06	0,41	-1,22	0,90
Pitch (deg)	-0,12	0,01	0,14	0,04	-0,77	0,36
Yaw (deg)	0,00	0,00	0,10	0,04	-1,01	-0,70
Mid cut Fx (N)	3,87E+06	4,25E+06	4,74E+06	1,16E+05	-0,50	0,30
Mid cut Fy (N)	-1,22E+06	-1,73E+03	1,33E+06	3,80E+05	-1,00	1,87
Mid cut Fz (N)	-1,24E+07	-1,05E+07	-8,52E+06	4,81E+05	-0,05	0,36
Mid cut Mx (Nm)	-1,13E+07	-6,34E+03	1,11E+07	3,45E+06	-0,96	1,47
Mid cut My (Nm)	-8,68E+08	-7,87E+08	-7,09E+08	2,33E+07	-0,04	0,03
Mid cut Mz (Nm)	-4,15E+07	1,41E+05	4,69E+07	1,43E+07	-1,81	9,21

A.5 S008

A.5.1 Condition 13

The experimental tests compared against are:

- Ser008-Test001-Run001
- Ser008-Test001-Run002
- Ser008-Test002-Run001

Table A.37: Properties for S008Cond13

Sea state	S008
Speed (Kts)	12
Wave direction (deg)	180
Significant wave height (m)	10,78
Wave period (s)	5

Table A.38: Statistical data of the experiment for S008Cond13

S008Cond13	Min	Mean	Max	Standard deviation
Wave elevation (m)	-4,886188587	-0,000440005	4,623520111	1,05
Surge (m)	-3,527043941	-0,072384064	1,350497768	0,65
Sway (m)	-0,504131399	0,000428228	0,699478278	0,17
Heave (m)	-1,105700269	0,078216529	0,968433559	0,28
Roll (deg)	-2,83	0,061005833	2,44	0,91
Pitch (deg)	-3,32	0,056951477	3,18	0,75
Yaw (deg)	-0,001393956	-0,001393956	0,695	0,18
Mid cut Fx (N)	6,07E+06	8,40E+06	1,31E+07	5,82E+05
Mid cut Fy (N)	-4,57E+06	-2,46E+06	-6,01E+05	4,19E+05
Mid cut Fz (N)	-1,76E+07	-1,14E+07	-2,56E+06	1,79E+06
Mid cut Mx (Nm)	-8,71E+06	-1,38E+05	1,03E+07	3,41E+06
Mid cut My (Nm)	-1,51E+09	-8,33E+08	7,55E+07	1,91E+08
Mid cut Mz (Nm)	-8,71E+06	-1,38E+05	1,03E+07	3,41E+06

Table A.39: Statistical data of the simulation for S008Cond13

S008Cond13	Min	Mean	Max	Standard deviation	Mean difference	Std. deviation difference
Wave elevation (m)	-3,78	0,00	3,56	1,25	6,60	0,19
Surge (m)	-0,87	0,29	1,37	0,38	-5,04	-0,41
Sway (m)	0,00	0,00	0,00	0,00	-1,00	-1,00
Heave (m)	-1,50	0,12	1,66	0,52	0,59	0,82
Roll (deg)	0,00	0,00	0,00	0,00	-1,00	-1,00
Pitch (deg)	-3,03	0,00	3,17	0,97	-1,00	0,30
Yaw (deg)	0,00	0,00	0,00	0,00	-1,00	-1,00
Mid cut Fx (N)	1,9E+06	4,3E+06	6,8E+06	7,48E+05	-0,49	0,28
Mid cut Fy (N)	-8,0E+01	-1,2E-01	8,2E+01	2,72E+01	-1,00	-1,00
Mid cut Fz (N)	-1,7E+07	-1,1E+07	-3,6E+06	1,83E+06	-0,07	0,02
Mid cut Mx (Nm)	-7,6E+02	3,7E+03	7,9E+03	1,32E+03	-1,03	-1,00
Mid cut My (Nm)	-1,4E+09	-7,9E+08	-2,1E+08	1,79E+08	-0,05	-0,07
Mid cut Mz (Nm)	-6,4E+03	-2,1E+00	5,9E+03	2,20E+03	-1,00	-1,00

A.5.2 Condition 14

The experimental tests compared against are:

- Ser008-Test003-Run001
- Ser008-Test004-Run001
- Ser008-Test005-Run001

Table A.40: Properties for S008Cond14

Sea state	S008
Speed (Kts)	12
Wave direction (deg)	150
Significant wave height (m)	10,78
Wave period (s)	5

Table A.41: Statistical data of the experiment for S008Cond14

S008Cond14	Min	Mean	Max	Standard deviation
Wave elevation (m)	-4,637393	-0,02781	3,494231	1,05
Surge (m)	-1,788602	0,112856	1,362791	0,63
Sway (m)	-1,146859	0,038615	1,712174	0,59
Heave (m)	-1,257244	0,06205	1,258971	0,40
Roll (deg)	-4,5	0,244239	3,555	1,47
Pitch (deg)	-3,18	0,062342	3,165	0,91
Yaw (deg)	-0,020823	-0,02082	2,055	0,58
Mid cut Fx (N)	6,44E+06	8,39E+06	1,15E+07	5,60E+05
Mid cut Fy (N)	-6,94E+06	-2,44E+06	1,08E+05	9,58E+05
Mid cut Fz (N)	-1,54E+07	-1,14E+07	-5,46E+06	1,31E+06
Mid cut Mx (Nm)	-2,63E+07	-1,19E+06	2,64E+07	7,79E+06
Mid cut My (Nm)	-1,45E+09	-8,31E+08	1,26E+07	1,81E+08
Mid cut Mz (Nm)	-2,63E+07	-1,19E+06	2,64E+07	7,79E+06

Table A.42: Statistical data of the simulation for S008Cond14

S008Cond14	Min	Mean	Max	Standard deviation	Mean difference	Std. deviation difference
Wave elevation (m)	-3,23	0,01	3,15	1,25	-1,19	0,19
Surge (m)	-0,50	0,29	1,05	0,34	1,56	-0,46
Sway (m)	-2,17	-0,04	1,77	0,65	-2,02	0,10
Heave (m)	-1,13	0,12	1,35	0,60	0,93	0,52
Roll (deg)	-2,96	0,00	2,91	1,28	-1,00	-0,13
Pitch (deg)	-2,00	0,01	2,02	1,15	-0,86	0,27
Yaw (deg)	0,03	0,03	0,77	0,26	-2,56	-0,55
Mid cut Fx (N)	2,6E+06	4,3E+06	5,9E+06	8,04E+05	-0,49	0,43
Mid cut Fy (N)	-1,8E+06	-2,1E+03	1,8E+06	8,04E+05	-1,00	-0,16
Mid cut Fz (N)	-1,4E+07	-1,1E+07	-6,7E+06	1,61E+06	-0,07	0,23
Mid cut Mx (Nm)	-1,8E+07	8,2E+03	1,7E+07	8,15E+06	-1,01	0,05
Mid cut My (Nm)	-1,2E+09	-7,9E+08	-4,2E+08	1,76E+08	-0,05	-0,03
Mid cut Mz (Nm)	-7,3E+07	-1,3E+05	6,9E+07	3,10E+07	-0,89	2,98

A.5.3 Condition 15

The experimental tests compared against are:

- Ser008-Test006-Run001
- Ser008-Test007-Run001

Table A.43: Properties for S008Cond15

Sea state	S008
Speed (Kts)	15
Wave direction (deg)	180
Significant wave height (m)	10,78
Wave period (s)	5

Table A.44: Statistical data of the experiment for S008Cond15

S008Cond15	Min	Mean	Max	Standard deviation
Wave elevation (m)	-3,053983478	-0,006511853	2,890278125	0,99
Surge (m)	-1,86897387	0,032752299	0,918541805	0,53
Sway (m)	-0,418435856	-0,008232846	0,34170971	0,11
Heave (m)	-0,716216622	0,116539405	0,842315376	0,30
Roll (deg)	-1,18	0,043712257	1,515	0,40
Pitch (deg)	-2,09	0,054220189	2,055	0,67
Yaw (deg)	0,006242963	0,006242963	0,355	0,15
Mid cut Fx (N)	7,16E+06	8,52E+06	1,03E+07	5,70E+05
Mid cut Fy (N)	-3,29E+06	-2,44E+06	-1,50E+06	2,98E+05
Mid cut Fz (N)	-1,54E+07	-1,13E+07	-6,01E+06	1,59E+06
Mid cut Mx (Nm)	-6,09E+06	-7,43E+04	6,39E+06	1,83E+06
Mid cut My (Nm)	-1,25E+09	-8,23E+08	-2,94E+08	1,69E+08
Mid cut Mz (Nm)	-6,09E+06	-7,43E+04	6,39E+06	1,83E+06

Table A.45: Statistical data of the simulation for S008Cond15

S008Cond15	Min	Mean	Max	Standard deviation	Mean difference	Std. deviation difference
Wave elevation (m)	-3,85	0,00	3,98	1,25	-0,70	0,26
Surge (m)	-0,68	0,29	1,06	0,31	7,75	-0,41
Sway (m)	0,00	0,00	0,00	0,00	-1,00	-1,00
Heave (m)	-1,42	0,12	1,61	0,58	0,06	0,90
Roll (deg)	0,00	0,00	0,00	0,00	-1,00	-1,00
Pitch (deg)	-2,59	0,00	2,54	1,02	-0,99	0,52
Yaw (deg)	0,00	0,00	0,00	0,00	-1,00	-1,00
Mid cut Fx (N)	1,9E+06	4,3E+06	6,5E+06	8,32E+05	-0,50	0,46
Mid cut Fy (N)	-6,8E+01	1,8E-01	7,6E+01	2,27E+01	-1,00	-1,00
Mid cut Fz (N)	-1,7E+07	-1,1E+07	-3,7E+06	1,85E+06	-0,06	0,16
Mid cut Mx (Nm)	-3,7E+02	3,8E+03	7,9E+03	1,46E+03	-1,05	-1,00
Mid cut My (Nm)	-1,3E+09	-7,9E+08	-2,4E+08	1,80E+08	-0,04	0,06
Mid cut Mz (Nm)	-5,8E+03	8,5E+00	5,4E+03	1,89E+03	-1,00	-1,00

A.5.4 Condition 16

The experimental tests compared against are:

- Ser008-Test008-Run001
- Ser008-Test009-Run001
- Ser008-Test010-Run001

Table A.46: Properties for S008Cond16

Sea state	S008
Speed (Kts)	15
Wave direction (deg)	150
Significant wave height (m)	10,78
Wave period (s)	5

Table A.47: Statistical data of the simulation for S008Cond16

S006Cond16	Min	Mean	Max	Standard deviation
Wave elevation (m)	-4,33403	-0,02526	3,279656	1,07
Surge (m)	-1,896738	0,072105	1,361832	0,70
Sway (m)	-0,925173	0,027112	1,029323	0,49
Heave (m)	-1,22484	0,097213	1,421339	0,39
Roll (deg)	-2,975	0,26816	3,09	1,05
Pitch (deg)	-3,025	0,060519	3,16	0,93
Yaw (deg)	0,0136194	0,013619	1,355	0,50
Mid cut Fx (N)	6,65E+06	8,57E+06	1,21E+07	6,48E+05
Mid cut Fy (N)	-5,97E+06	-2,42E+06	6,47E+05	9,45E+05
Mid cut Fz (N)	-1,62E+07	-1,12E+07	-4,84E+06	1,41E+06
Mid cut Mx (Nm)	-2,59E+07	-1,21E+06	1,99E+07	7,14E+06
Mid cut My (Nm)	-1,35E+09	-8,18E+08	2,24E+07	1,92E+08
Mid cut Mz (Nm)	-2,59E+07	-1,21E+06	1,99E+07	7,14E+06

Table A.48: Statistical data of the simulation for S008Cond16

S006Cond16	Min	Mean	Max	Standard deviation	Mean difference	Std. deviation difference
Wave elevation (m)	-3,15	0,00	3,16	1,25	-1,19	0,17
Surge (m)	-1,14	0,25	1,58	0,48	2,47	-0,31
Sway (m)	-1,37	0,04	1,49	0,57	0,33	0,15
Heave (m)	-1,23	0,12	1,49	0,69	0,21	0,75
Roll (deg)	-3,24	0,00	3,19	1,42	-0,99	0,35
Pitch (deg)	-2,18	0,01	2,18	1,23	-0,85	0,33
Yaw (deg)	0,01	0,01	0,68	0,25	-0,15	-0,50
Mid cut Fx (N)	2,5E+06	4,3E+06	6,1E+06	9,03E+05	-0,50	0,39
Mid cut Fy (N)	-1,8E+06	-3,5E+02	1,8E+06	8,58E+05	-1,00	-0,09
Mid cut Fz (N)	-1,5E+07	-1,1E+07	-6,6E+06	1,65E+06	-0,06	0,17
Mid cut Mx (Nm)	-2,0E+07	3,7E+03	2,0E+07	9,60E+06	-1,00	0,35
Mid cut My (Nm)	-1,2E+09	-7,9E+08	-4,1E+08	1,79E+08	-0,03	-0,07
Mid cut Mz (Nm)	-6,8E+07	2,6E+04	6,9E+07	3,01E+07	-1,02	3,21

